Large-scale seroepidemiology uncovers nephrological pathologies in people with tau autoimmunity

Authors:

Andreia D. Magalhães[1†], Marc Emmenegger[1&], Elena De Cecco[1], Manfredi Carta[1‡], Karl Frontzek[1§], Andra Chincisan[1‖], Jingjing Guo[1], Simone Hornemann[1*], Adriano Aguzzi[1*]

Affiliations:

[1] Institute of Neuropathology, University of Zurich; CH-8091 Zurich, Switzerland

[*] Correspondence: simone.hornemann@usz.ch and adriano.aguzzi@usz.ch

[†] Present address: Department of Neurology, Inselspital, Bern University Hospital; CH-3010 Bern, Switzerland

[&] Present address: Division of Medical Immunology, Department of Laboratory Medicine, University Hospital Basel; CH-4031 Basel, Switzerland

[‡] Present address: Institute of Neurology, University of Zurich; CH-8091 Zurich, Switzerland

[§] Present address: University College London, Institute of Neurology, Queen Square Brain Bank; WC1N 1PJ London, United Kingdom

[‖] Present address: Credit Suisse; CH-8001 Zurich, Switzerland

One Sentence Summary:

Anti-tau autoantibodies are prevalent, increase with age, and are associated with kidney and urinary disorders.

Abstract:

Intraneuronal aggregates of the microtubule-associated protein tau play a pivotal role in Alzheimer's disease and several other neurodegenerative syndromes. Anti-tau antibodies can reduce pathology in mouse models of neurodegeneration and are currently being tested in humans. Here, we performed a large-scale seroepidemiological search for anti-tau IgG autoantibodies (ατ) on 40,497 human plasma samples. High-titer $\alpha\tau^+$ individuals were surprisingly prevalent, with hospital patients being three times more likely to be $\alpha\tau^+$ ($EC_{50} \geq 2^6$) than healthy blood donors (4.8% vs 1.6%). Their autoantibodies bound selectively to tau, inhibited tau aggregation *in vitro*, and interfered with tau detection in plasma samples. No association was found between ατ autoantibodies and neurological disorders. Instead, tau autoreactivity showed a significant association with kidney and urinary disorders (adjusted RR 1.27, 95% CI 1.10-1.45, P=0.001 and 1.40, 95% CI 1.20-1.63, P<0.001 respectively). These results identify a previously unrecognized association between ατ autoimmunity and extraneural diseases, inform clinical trials of anti-tau immunotherapies about potential untoward effects, and uncover a prevalent confounder of immunoassay tau measurements in plasma.

Main Text:

INTRODUCTION

Tau is a microtubule binding protein expressed in neurons and involved in cytoskeletal dynamics (*1, 2*). It plays a pivotal role in a variety of neurodegenerative diseases, including Alzheimer's disease (AD) (*3*), progressive supranuclear palsy, and various syndromes collectively referred to as tauopathies (*4*). The presence of brain neurofibrillary tau tangles correlates with cognitive decline (*5*), and plasma measurements of total and phosphorylated tau have emerged as promising biomarkers for the detection and monitoring of AD progression (*6-9*). Moreover, active and passive immunization with antibodies against a wide range of tau epitopes can reduce pathology and functional decline in animal models of tauopathies (*10, 11*) and are being tested in clinical trials of neurodegenerative diseases (*12*).

Natural autoantibodies are immunoglobulins generated against self-antigens in the absence of external antigen stimulation (*13*). They are a normal part of the immunoglobulin repertoire and have physiological roles in homeostasis and surveillance, including the clearance of cellular debris, anti-inflammatory activity, and first-line defense against pathogens (*14*). However, in certain situations, natural autoantibodies can also cause pathological autoimmunity. The study of natural autoantibodies can therefore inform about properties of their targets, e.g. unrecognized protective or contributing roles in disease (*15*). Some natural autoantibodies can cause neurological disorders, such as antibodies targeting the N-methyl-D-aspartate receptor (NMDAR) in encephalitis (*16*) or antibodies targeting aquaporin-4 (AQP4) in neuromyelitis optica (*17*). Conversely, natural antibodies against amyloid-β have been suggested to protect and slow the progression of AD; aducanumab, a monoclonal antibody developed from B-cells of cognitively normal older age individuals, has been studied as a treatment for AD (*18*).

Anti-tau autoantibodies have been detected in plasma of patients with AD (*19*) and Parkinson's disease (*20*), but also in non-neurodegeneration controls. The effects, if any, of natural anti-tau autoantibodies in modulating the risk of developing neurodegenerative diseases are unknown. The study of individuals with anti-tau autoantibodies could clarify their potential as modifiers or biomarkers of disease. Here, we tested 40,497 plasma samples from healthy blood donors and from patients admitted to a university hospital in the frame of a two-sites cross-sectional study. We found that anti-tau autoimmunity is highly specific and surprisingly frequent, with its prevalence

increasing with age. Unexpectedly, natural anti-tau autoantibodies were associated with a previously unrecognized syndrome comprising kidney and urinary disorders.

RESULTS

Prevalence of naturally occurring plasma anti-tau autoantibodies

We used a cross-sectional study design to assess naturally occurring IgG autoantibodies against the microtubule-binding domain of the tau protein (MTBD-tau). Plasma samples from 32,291 patients (age ≥ 18 years) from an unselected university hospital cohort and from 8,206 healthy blood donors were screened for anti-MTBD-tau plasma IgG autoantibodies with a miniaturized ELISA (Enzyme-Linked Immunosorbent Assay) in 1,536-well microplates using acoustic dispensing (*21-23*). Each plasma sample was tested at eight serial two-fold dilutions (1:50 to 1:6,000). Optical-density readings were fitted by logistic regression from which the inflexion points were derived. Antibody titers were defined as "$-\log_{10}(EC_{50})$", i.e. the negative decadic logarithm of the plasma dilution factor corresponding to the inflexion point of the respective regression curve.

After exclusion of non-informative samples (fitting error >20% $-\log_{10}(EC_{50})$ or high background), we included 24,339 patients' samples and 6,590 healthy blood donors' samples in the analysis (Fig. 1A). A titer of $-\log_{10}(EC_{50}) \geq 1.8$, approximately corresponding to a nominal dilution of > 1/64, was selected as a cutoff to call tau-autoreactive samples (henceforth named $\alpha\tau^+$). Using these parameters, 4.80% (n=1,169) of 24,339 patients' samples, but only 1.58% (n=104) of 6,590 healthy donors were $\alpha\tau^+$ (Fig. 1A-C). These data are indicative of a much higher prevalence of anti-tau immunoreactivity in unselected hospital patients than in healthy individuals (P<0.001).

Demographic data was available for 4,157 of the 6,590 blood donors included in the study. Their median age was 42 years (interquartile range [IQR] 29-54), whereas the median age of hospital patients was 55 years (IQR: 40-69) (P<0.001). Of the healthy blood donors, 40.9% (n=1,698) were women, whereas for the hospital group, 47.7% (n=11,609) of the patients were women (P<0.001). Using a multivariate log-binomial regression model (*24, 25*) adjusted for age and sex, we found that hospital patients had 2.3 times the risk of healthy donors to be $\alpha\tau^+$ (adjusted RR 2.30, 95% confidence interval (CI) 1.83-2.92, P<0.001, Fig. 1D).

The replicability of the microELISA screen was evaluated by testing 308 randomly picked samples in duplicate, and was found to be high (R^2=0.84, P<0.001, Fig. 1E). To estimate any nonspecific cross-reactivity, we determined the immunoreactivity to two other proteins implicated in neurodegeneration, amyloid-ß pyroglutamate and the cellular prion protein (PrP^C) (*22*). Of 12,297 patient samples, 604 samples were positive against MTBD-tau and 5 against amyloid-ß pyroglutamate but none was cross-reactive against both targets (P=1, χ^2 test) (Fig. 1F), Moreover, of 13,099

patient samples, 694 were reactive against MTBD-tau and 15 against PrP^C, but again none was cross-reactive against both targets (P=0.734, χ^2 test) (Fig. 1G)

Characterization of $\alpha\tau^+$ samples

Anti-tau autoantibodies were purified by MTBD-tau affinity chromatography from four individual $\alpha\tau^+$ patients (P1-P4) and from a pool of six $\alpha\tau^+$ samples for which larger sample volumes were available. Their half-maximal effective concentration (EC_{50}) to MTBD-tau was determined by indirect ELISA and compared to the EC_{50} of the well-characterized monoclonal anti-MTBD-tau antibody, RD4 (dissociation constant K_d=570 nM) (*26*). At equal concentrations, RD4 displayed binding to MTBD-tau with EC_{50}=0.002 µg/ml Fig. 2A and no binding to MTBD-tau-free plates, whereas the five purified autoantibody samples had EC_{50} values of 0.042-14.45 µg/ml (Fig. 2A). As expected, no binding to MTBD-tau was observed for the unrelated antibody, Relatlimab (anti-LAG3) (*27*) (Fig. 2A).

To probe the binding specificity of the purified $\alpha\tau^+$ autoantibodies, we performed a soluble-competition immunoassay with MTBD-tau (Fig. 2B). This is a stringent assay which, when positive, identifies high-affinity interactions. Purified autoantibodies from four $\alpha\tau^+$ patients and control were pre-incubated with either recombinant MTBD-tau, a pool of eight synthetic 25-meric peptides overlapping with each other by 10 residues and covering the MTBD-tau sequence, an unrelated synthetic 25-meric peptide derived from TREM2 (Triggering Receptor Expressed on Myeloid Cells 2), or albumin. Each antigen was tested for its capability to impair the binding of purified $\alpha\tau^+$ autoantibodies to plate-bound MTBD-tau by ELISA. Pre-incubation with MTBD-tau and pooled MTBD-tau peptides, but not with the TREM2 peptide or albumin, decreased the ELISA signal in a concentration-dependent manner (Fig. 2C). These results confirm the binding specificity of $\alpha\tau^+$ plasma for MTBD-tau.

Certain antibodies can display broad polyreactivity which may raise doubts about their specificity. To probe for polyreactivity of purified $\alpha\tau^+$ autoantibodies, we performed indirect ELISA assays against a variety of structurally different unrelated self-antigens and non-self-bacterial antigens, including MTBD-tau, albumin, cardiolipin, DNA, insulin, and lipopolysaccharides (LPS) as well as with uncoated plates. Purified anti-tau autoantibodies were reactive against MTBD-tau but not against any of the tested antigens (Fig. 2D).

We then tested the purified $\alpha\tau^+$ autoantibodies by immunofluorescence staining and Western blotting. Purified anti-tau autoantibodies staining co-localized to cytoplasmic EGFP-0N4RTau in SH-SY5Y cells and showed similar specific binding to anti-tau mouse monoclonal antibody HT7, but not to non-transfected cells (Fig. 2E). Western blot analysis confirmed that purified $\alpha\tau^+$ autoantibodies detected tau-specific bands in cell lysates of SH-SY5Y cells overexpressing $tau^{P301L/S320F}$, but not in wild-type (wt) SH-SY5Y cells (Fig. 2F and Fig. S1). These data provide substantial evidence that the immunoreactivity observed in $\alpha\tau^+$ samples is indeed highly specific for tau.

We further investigated the subclass composition of immunoglobulin heavy and light chains of 13 $\alpha\tau^+$ plasma samples. All four IgG subclasses were found, with IgG1 being detected in all 13 samples, followed by IgG3 in 12 samples, IgG2 in 11 samples and IgG4 in 8 samples (Fig. 2G). κ light chains were detected in 9 samples and λ light chains in 7 samples (Fig. 2H). Three samples were polytypic for κ and λ (Fig. 2H).

We then profiled the epitopes recognized by the MTBD-tau autoantibodies in $\alpha\tau^+$ plasmas and of MTBD-tau affinity chromatography purified autoantibodies from five $\alpha\tau^+$ samples (P2-P6) using a library of 8 synthetic 25-meric peptides with 10 residues of overlap covering the sequence of MTBD-tau. Most samples showed reactivity to peptides 3 (11 of 14) and 5 (10 of 14) which correspond to the repeat regions 2 and 3 of MTBD-tau (Figs 2I and S2). A polyclonal antibody response was identified in at least 7 of 13 samples based on light-chain typing and epitope mapping (Fig. 2G-H). Taken together, these findings confirm the presence of naturally occurring antibodies of different subclasses, light chains and against different epitopes of MTBD-tau in $\alpha\tau^+$ plasma samples.

Biological activity of $\alpha\tau^+$ autoantibodies

Anti-tau antibodies can antagonize the aggregation of tau into pathogenic assemblies (*28*). To investigate whether plasma MTBD-tau autoantibodies interfere with the aggregation of MTBD-tau, MTBD-tau affinity purified autoantibodies from two further $\alpha\tau^+$ samples (P7 and P8) were subjected to an *in vitro* tau aggregation assay (*28*). MTBD-tau aggregation was induced by heparin and shaking and monitored using thioflavin T (ThT) (Fig. 3A). The presence of the anti-MTBD-tau autoantibodies reduced the plateau of the ThT fluorescence signal in the kinetic trace by about half, whereas antibodies purified by protein G affinity chromatography from an $\alpha\tau^-$ patient had no

effect (Fig. 3A). These findings indicate that $\alpha\tau^+$ autoantibodies inhibit MTBD-tau aggregation *in vitro*

Plasma tau is considered a possible biomarker for the progression of several neurological diseases (*6-9, 29*). To probe for an interference of $\alpha\tau^+$ autoantibodies in plasma tau immunoassays, we added tau^{441} to the plasma of healthy donors and examined the effect of $\alpha\tau^+$ autoantibodies onto tau detection (Fig. 3B). Purified anti-MTBD-tau autoantibodies from 5 individual $\alpha\tau^+$ patients (P2-P6) were added to tau^{441}-spiked plasma. After incubation, the amount of free tau^{441} was analyzed by ELISA using the commercial anti-tau BT2 as a capture antibody (epitope on human tau^{441}: residues 194-198) and ab64193 as a detection antibody (epitope on human tau^{441} surrounding residue 262 (*30*)). We observed that purified anti-tau autoantibodies, P4-P6, induced a concentration-dependent impairment of detection of tau^{441} (Fig. 3C-D) hampering the detection of plasma-spiked tau^{441} by up to approximately tenfold at higher anti-MTBD-tau autoantibodies concentrations (Fig. 3C-D). In contrast, P2-P3 did not show any significant impairment of the detection of plasma-spiked tau^{441}. This variability of interference is explained by the binding epitopes on tau^{441}. P4-P6 occupy tau residues 244 to 282 which include the epitope of the detection antibody ab64193, whereas P2-P3 occupy residues 273 to 327 which are outside the binding epitope of ab64193 (Fig. S2). We thus conclude that the presence of $\alpha\tau^+$ autoantibodies may interfere with the detection of plasma tau in immunoassays depending on the combination of epitopes of the patient samples and of the commercial antibodies used in the immunoassay.

Demographic characteristics of tau-immunoreactive patients

We performed univariate logistic regression analyses of basic demographic data available in the electronic health records for the 24,339 hospital patients. The age of $\alpha\tau^+$ patients (median: 58 years; IQR: 43-71) was significantly higher than that of $\alpha\tau^-$ (median: 55; IQR: 40-68; $P < 0.001$, Fig. 4A). A more detailed breakdown of the date showed that the prevalence of $\alpha\tau$ immunoreactivity increased with age, from 3.9% in patients aged <29 years to 7.6% in patients older than 90 years ($P<0.001$, Fig. 4B). A log-binomial regression model (*24, 31*) estimated that the risk ratio for the presence of anti-MTBD-tau autoantibodies was highest for patients aged 70-99 years (RR 1.26, 95%CI 1.11-1.43, $P<0.001$, Fig. 4C) and for women (RR 1.20, 95%CI 1.07-1.39, $P=0.002$, Fig. 4C). Due to the association of anti-MTBD-tau autoantibodies with increased age and female sex,

all further risk ratios were calculated using a multivariate log-binomial regression model adjusted for age and sex [age-and-sex adjusted risk ratio (aRR)].

Any possible correlations between $\alpha\tau^+$ and admission to specific clinical departments might inform on potential associations with specific diseases. The highest age-and-gender adjusted risk ratios for $\alpha\tau^+$ were found for the departments of angiology (RR 1.84, 95%CI 1.21-2.63, P=0.002) and nephrology (RR 1.50, 95%CI 1.16-1.89, P=0.001, Fig. 4D-E). Importantly, no significant difference was found between the percentage of $\alpha\tau^+$ and $\alpha\tau^-$ patients from the department of neurology (Fig. 4D).

Neurological disorders and anti-tau autoimmunity

We next mined pseudonymized clinical data pertaining to the diagnoses of 23,375 patients as represented by ICD-10 codes (International Classification of Disease and Related Health Problems, 10th revision) (Fig. 5A). Given the involvement of tau in neurodegenerative diseases (3), we focused on evaluating the association between anti-MTBD-tau autoantibodies and neurological disease, which we categorized in 23 main groups of disorders. No associations between $\alpha\tau$+ and neurological diseases were identified (Fig. 5A). To further validate this finding, we performed a targeted screen using plasma samples from 47 patients with AD and 68 similarly aged non-AD patients selected from our plasma biobank (Table S1). Samples were tested for anti-MTBD-tau IgG autoantibodies, as in the primary screen, and additionally for anti-MTBD-tau IgA autoantibodies and anti-full-length tau IgG and IgA autoantibodies. No significant difference in reactivity was observed between the plasma samples from AD patients and non-AD controls (Fig. 5B), supporting the hypothesis that the presence of autoantibodies targeting MTBD-tau is unrelated to AD or other neurological disorders.

Systemic disorders and anti-tau autoimmunity

We next assessed possible associations between tau autoimmunity and extraneural diseases, which we binned into 27 main groups of disorders (Fig. 6A). After adjustment for multiple comparisons, $\alpha\tau$ immunoreactivity showed significant associations with vascular disorders (adjusted RR 1.51, 95%CI 1.28-1.77, P<0.001), nutritional disorders (adjusted RR 1.31, 95%CI 1.14-1.50, P<0.001), anemia (adjusted RR 1.49, 95%CI 1.21-1.82, P<0.001), kidney disorders (adjusted RR 1.27, 95%CI 1.10-1.45, P=0.001) and urinary disorders (adjusted RR 1.40, 95%CI 1.20-1.63, P<0.001)

(Fig. 6B), whereas no association was observed among patients with autoimmune disorders (Fig. S3). There was no difference in the coincidence of all comorbidities between the $\alpha\tau^+$ samples (5, 0.46%) and the $\alpha\tau^-$ samples (69, 0.33%) (P=0.633).

To address potential biases arising from grouping and selecting major categories, we further explored the association between $\alpha\tau^+$ and individual ICD-10 codes. Across 276 individual ICD-10 codes and after correction for multiple comparisons, eight exhibited significant associations with $\alpha\tau^+$ (Fig. 6B-C). These included "E61 – deficiency of other nutrient elements" (adjusted RR 2.22, 95%CI 1.54-3.06, P<0.001), "I74 - arterial embolism and thrombosis*"* (adjusted RR 2.09, 95%CI 1.40-2.94, P<0.001), "N30 – cystitis" (adjusted RR 1.84, 95%CI 1.32-2.47, P<0.001), "I70 – atherosclerosis*"* (adjusted RR 1.57, 95%CI 1.29-1.89, P<0.001), "D50 – iron deficiency anemia*"* (adjusted RR 1.50, 95%CI 1.21-1.82, P<0.001), "N39 – other urinary disorders" (adjusted RR 1.40, 95%CI 1.19-1.64, P<0.001), "B96 – other bacterial agents as the cause of diseases*"* (adjusted RR 1.40, 95% CI 1.17-1.66, P<0.001) and "N18 – chronic kidney disease*"* (adjusted RR 1.38, 95%CI 1.18-1.60, P<0.001) (Fig. 6C). Again, it is well-known that many of these diseases are often co-incident in clinical practice. Conversely, we found no significant negative association between tau autoreactivity and any ICD-10 codes that could suggest a decreased risk for a specific disease in $\alpha\tau^+$ patients (Fig. 6B).

To further verify the association between $\alpha\tau^+$ and individual ICD-10 codes, we used a different statistical approach. Instead of using a titer of $-\log_{10}(EC_{50}) \geq 1.8$ to dichotomize samples as positives and negatives, we performed a Bayesian logistic regression using logit-transformed EC_{50} values ($-\text{logit}[EC_{50}]$) as a continuous outcome. We could verify that all the previously referred eight ICD-10 codes showed positive associations with $-\text{logit}[EC_{50}]$ (Fig. 6D).

With the aim of further validating these conditions as clinically significant associations with plasma MTBD-tau IgG autoantibodies, we examined the association between $\alpha\tau^+$ and 106 commonly requested laboratory parameters using data available for 24,177 patients. This analysis was independent of any ICD-10 classifiers. After correction for multiple comparisons, the laboratory markers "Leukocytes, urine", "Potassium" and "Urea" were positively associated with tau autoimmunity (Fig. 6E). The association with increasing levels of urea and potassium suggest a link to kidney failure, whereas leukocytes in urine are a feature of urinary tract infections. These findings are therefore in good agreement and provide a strong independent line of evidence for the hypothesis that anti-tau autoimmunity correlates with such disorders.

Comparing the prevalence of kidney and urinary disorders in $\alpha\tau^-$ and $\alpha\tau^+$ patients, we identified an excess prevalence of chronic kidney disease of 5.3% in $\alpha\tau^+$ patients (12.4% in $\alpha\tau^-$ and 17.7% in $\alpha\tau^+$), an excess prevalence of cystitis of 1.7% in $\alpha\tau^+$ patients (1.6% in $\alpha\tau^-$ and 3.3% in $\alpha\tau^+$), and an excess prevalence of other urinary disorders of 4.8% (10.3% in $\alpha\tau^-$ and 15.1% in $\alpha\tau^+$) (Fig. 6F). These data further support the hyperprevalence of tau autoimmunity in patients with these diseases.

DISCUSSION

Due to their hypothesis-free character and their independence from priors, large-scale seroepidemiological screens have the potential to uncover disease correlations and new biological effects of its targets that may not be discoverable in any other way. Such screens are suited to identifying pathologies correlating with any immunoreactivity, but require economical, massively parallel assays. Using acoustic dispensing and extensive customized automation, we miniaturized antibody detection to a volume of 3 µl/sample and to 1,536-well microplates. This allowed us to run 40,000 assays/24 hrs using a robotic platform. In total, we performed >300,000 immunoassays on >40,000 plasma samples obtained from university hospital patients and healthy blood donors for ατ autoreactivity (*21-23*). ELISA miniaturization lowered the cost of individual assays, allowing us to measure eight data points across a dilution range of 1:50 to 1:6,000 for each sample. Consequently, this method enables us to determine autoantibody titers more stringently and unambiguously (*21-23*).

Even after adjustments for age and sex, the $\alpha\tau^+$ rate in hospital patients was three-fold higher than in healthy blood donors and was 2.4 times higher than that of autoantibodies targeting other intracellular neuronal targets reported by others (*32*). Plasma ατ IgG correlated with female sex and increased with age. The specificity of $\alpha\tau^+$ plasma to MTBD-tau was high and was confirmed by multiple orthogonal assays including epitope mapping. Most $\alpha\tau^+$ samples were polyclonal, and all IgG subclasses were represented. Purified ατ autoantibodies exhibited the capability to inhibit MTBD-tau aggregation *in vitro*. Finally, it was possible to compete them by MTBD-tau and a pool of synthetic MTBD-tau peptides, but not by other antigens.

The much higher prevalence of ατ positivity in hospital patients than in healthy blood donors suggests that tau autoreactivity is low in healthy populations and that ατ autoantibodies are associated with disease. However, we did not find any association between $\alpha\tau^+$ and any neurological conditions including neurodegenerative diseases. This observation is compatible with reports of similar levels of plasma tau autoantibodies in Alzheimer's disease patients and non-demented controls (*33*). Instead, we uncovered a robust and specific association between plasma anti-MTBD-tau IgG autoantibodies and the diagnosis of kidney and urinary disorders, which was validated by the independent finding of association between ατ immunoreactivity and higher prevalence of positive

samples from the department of Nephrology, grouped kidney and urinary diseases, individual kidney and urinary diagnosis codes as well as high serum urea and potassium and high urine leukocytes, which are clinical laboratory biomarkers of kidney and urinary disorders.

This seroepidemiological studies cannot establish causality: hence ατ seropositivity could be a cause or a consequence of the clinical syndromes associated with it. Indeed, some patients with frontotemporal dementia and Parkinsonism caused by mutant tau experience urinary incontinence (*34*) which may plausibly result from neuronal pathologies. However, tau is expressed in extraneural tissues, including kidney podocytes and urinary bladder (*2, 35-37*), and its ablation causes glomerular pathologies (*38*). Besides raising the possibility that plasma ατ autoantibodies might drive kidney pathologies, these findings suggest that such autoantibodies represent useful biomarkers of these diseases. Finally, these findings suggest that it will be important to monitor renal and urinary function in the current clinical trials of tau immunotherapy (*39-41*).

Recent studies have explored the use of total and phosphorylated tau measurements in plasma as biomarkers for AD diagnosis and for monitoring its progression (*6-9, 29, 42-46*). Measurement of plasma tau levels may enter regular clinical use as an easily accessible biomarker of AD. However, we found that anti-MTBD-tau autoantibodies could hinder tau detection in plasma by binding to epitopes recognized by commercial biomarker immunoassays. This aligns with prior research indicating that both plasma anti-tau autoantibodies and administered anti-tau antibodies can influence the dynamics of tau levels in plasma (*47*). Additionally, a recent community cohort study using an immunoassay for AD screening revealed associations between plasma tau levels and numerous comorbidities, with chronic kidney disease showing one of the strongest associations (*48*). These results imply that the presence of anti-tau autoantibodies in plasma might impact the effectiveness of plasma tau as an AD biomarker, particularly for patients with kidney or urinary diseases. This consideration may become crucial as plasma tau levels move toward routine clinical use in AD diagnosis.

Our large-scale assessment of plasma tau autoimmunity has certain limitations. Firstly, most samples analyzed in our study came from a university hospital cohort, implying a bias towards complex pathologies and polymorbidities. To account for this, we included a vast collection of samples from healthy blood donors. Secondly, our study is confined to two sites within a single region with approximately 1,500,000 inhabitants whose ethnic composition was not thoroughly examined. Additionally, a direct comparison of the prevalence of plasma anti-tau antibodies in these two cohorts

may potentially suffer from variations in materials, collection methods, and handling processes at the two different sites. Thirdly, our study is restricted to the analysis of specific disease groups and the absence of a longitudinal disease cohort that would allow for examining a time course, origin, and causal role of these autoantibodies. Finally, we used bacterially expressed MTBD-tau as target, thereby excluding full-length or post-translationally modified tau epitopes. As a result, plasma anti-tau autoantibodies associated with AD pathology might be missed, and our methodology may underestimate the prevalence of total anti-tau autoantibodies.

In conclusion, our study found a high seroprevalence of anti-MTBD-tau IgG autoantibodies in both plasma samples from university hospital patients and healthy blood donors. Tau autoimmunity is associated with female sex, older age and previously unrecognized extraneural diseases. These findings point to unrecognized roles for tau and anti-tau autoantibodies in extraneural pathologies and call for attentive clinical monitoring of such diseases in clinical trials of tau-targeting therapies and in the use of plasma tau as a biomarker of disease.

MATERIALS AND METHODS

Study design

Collection of samples and clinical data were conducted according to study protocols approved by the Cantonal Ethics Committee of the Canton of Zurich, Switzerland (KEK-ZH Nr. 2015-0561, BASEC-Nr. 2018-01042, and BASEC-Nr. 2020-01731). From December 2017 until February 2020, residual heparin plasma samples were obtained from the Department of Clinical Chemistry, University Hospital of Zurich), Switzerland. Blood samples were collected during routine clinical care from patients admitted either as inpatients or outpatients and were only included if basic demographic data was available, age was ≥ 18 years, and an informed consent for research had been provided. From March until July 2020, EDTA plasma samples were obtained from the Blood Donation Center of Zurich, Switzerland from blood donors according to standard criteria of blood donation. Exclusion criteria were as shown previously (*21*). Plasma samples were biobanked in 384-well plates at the Institute of Neuropathology, University of Zurich and tested on an automated indirect microELISA high-throughput platform for natural IgG autoantibodies against the microtubule-binding-domain of tau (MTBD-tau, tauK18, for details see (*21, 22*) and below).

Demographic and clinical data for the hospital cohort was obtained from clinical electronic records of the University Hospital of Zurich with follow-up until December 2021, while detailed clinical data for the blood donor cohort were not available for this study.

For the AD targeted screen, the AD patients and non-neurodegeneration controls were selected from the biobank of samples at the Institute of Neuropathology, USZ, using *International Statistical Classification of Diseases and Related Health Problems, Tenth Revision* (ICD-10) codes. AD patients were defined using ICD-10 code F00 or G30 and non-neurodegeneration controls were defined by the lack of any Fxx or Gxx ICD-10 codes.

Automated microELISA screen

Plasma samples were tested for natural anti-MTBD-tau IgG autoantibodies in a microELISA screen (*21-23*). Briefly, high-binding 1,536-well plates (Perkin Elmer, SpectraPlate 1536 HB) were coated with 1 µg/mL of in-house produced MTBD-tau (see protocol below) at 37 °C for 60 min. Plates were washed 3x with phosphate-buffered saline 0.1% Tween®20 (PBST) using a Biotek El406 washer-dispenser. Plates were blocked for 90 min with 5% milk (Migros) in PBST. Plasma was diluted 1:20 in 1% milk in PBST and dispensed into the MTBD-tau-coated plates using ultrasound dispensing with an ECHO 555 Liquid Handler (Labcyte/Beckman Coulter) and

in different volumes to a final volume of 3 µL/well and testing each sample at eight serial two-fold dilutions (1:50 to 1:6,000). Human IgG-depleted serum (MyBioSource) was used as negative control and anti-tau RD4 (4-repeat isoform) mouse monoclonal antibody (05-804 clone 1E1/A6 Merck Millipore) as a positive control. Samples were incubated for 120 min at room temperature (RT) after which plates were washed 5x with PBST. Secondary antibody peroxidase AffiniPure® goat anti-mouse IgG H+L (115-035-003, Jackson ImmunoResearch) at 1:2,000 dilution in 1% milk PBST for the RD4 positive control, and peroxidase AffiniPure® goat anti-human IgG Fcγ-specific (109-035-098, Jackson ImmunoResearch) 1:4,000 dilution in 1% milk PBST for the plasma samples and the IgG-depleted serum negative control were dispensed into the plates using a Biotek MultifloFX dispenser. Secondary antibodies were incubated for 60 min at RT after which plates were washed 3x with PBST. 3,3',5,5'-Tetramethylbenzidine (TMB) Chromogen Solution for ELISA (Invitrogen) was added to the plates as colorimetric horseradish peroxidase (HRP) substrate and incubated for 3 min at RT. Finally, 0.5 M H_2SO_4 was added to stop the reaction. Plates were briefly centrifuged after each dispensing step except after dispensing of TMB. Plates were read at Optical Density (OD) = 450 nm in a plate reader (Perkin Elmer, Envision).

For the replicability assessment, 308 samples were tested in duplicates using the same protocol as described before, and running the replicates on the same day but using different 1536-well assay (destination) plates, different plate coordinates for each replicate, and calculating the $-\log_{10}(EC_{50})$ of each replicate independently.

Non-specific cross-reactivity was assessed by testing plasma samples against against-MTBD-tau and amyloid-ß pyroglutamate (13,099 hospital patients' plasma samples) and the cellular prion protein (PrP^C) (12,297 hospital patients' samples) using a similar protocol as described above.

Production and purification of recombinant tau

The gene encoding the human truncated 4R-tau corresponding to the microtubule binding domain of tau protein (MTBD-tau) was cloned into a pRSET-A plasmid (Invitrogen). For protein expression the respective vector was transformed into *E.coli* BL21(DE3) cells. Bacterial cells were grown in Luria Broth (LB) medium (Invitrogen) at 37 °C until an OD_{600} of 0.8 was reached and were then induced with isopropyl-β-D-thiogalactoside (IPTG) at a final concentration of 1 mM. After growing the cells for additional 6 h at 37 °C, cultures were harvested by centrifugation (6,000*g*, 10 min, 4 °C). Pellets were suspended in 20 mM piperazine-N,N-bis(2-ethanesulfonic) acid (PIPES), pH 6.5, 1 mM ethylenediaminetetraacetic acid (EDTA) and 50 mM 2-mercaptoethanol buffer and

sonicated for 30 min at 4 °C. NaCl to 500 mM final concentration was added, samples were boiled at 95 °C for 20 min and centrifuged (9,000*g*, 30min, 4 °C). Ammonium sulfate was slowly added to a final concentration of 55% m/v and stirred for 1 h at room temperature (RT). Samples were centrifuged (15,000*g*, 10min, 4 °C), pellets were resuspended in 20 mM 4-(2-hydroxyethyl)piperazine-1-ethanesulfonic acid (HEPES) (pH 7.0), 2 mM dithiothreitol (DTT), passed through a 0.45 µm Acrodisc® filter (Sigma) and loaded onto Sepharose SP Fast Flow resin (Cytiva). Tau was eluted using a linear salt gradient from 0 to 1 M NaCl in 20 mM HEPES, pH 7.0, 2 mM DTT. Fractions containing tau were concentrated using Amicon® Ultra-15 centrifugal filter unit (10-kDa MWCO) (Merck) and dialyzed overnight at 4°C against phosphate-buffered saline (PBS) (pH 7.4) (Kantonsapotheke Zurich), 1mM DTT. Pooled samples were passed through a HiLoad 26/60 Superdex75 (GE Healthcare) column. Protein samples were analyzed by SDS-PAGE and samples containing tau were concentrated using an Amicon® Ultra-15 centrifugal filter unit (10-kDa MWCO). Samples were assessed by SDS-PAGE and electrospray ionization-mass spectrometry (Functional Genomics Center Zurich, Switzerland). Pure MTBD-tau samples were stored until further use at -80°C. The concentration of tau was determined using a bicinchoninic acid assay (Pierce BCA Protein Assay Kit, Thermo Fisher).

For the purification of full-length tau, a similar protocol was used with the following changes. The gene encoding the longest 4R isoform of human full-length tau protein, tau^{441}, (tau/pET29b, Addgene #16316, gift from Peter Klein (*49*)) was cloned into a pRSET-A plasmid (Invitrogen). For protein expression, E.*coli* BL21(DE3)pLysS cells were transformed with the pRSET-A plasmid encoding tau^{441}. Cells were grown in Overnight Express™ Instant TB media (Novagen) for 6 h at 37 °C and then 12 h at 25 °C. Fractions containing full-length tau were concentrated using Amicon® Ultra-15 centrifugal filter unit (30-kDa MWCO) (Merck).

Purification of anti-tau autoantibodies from patient samples

Heparin plasma (between 3 mL and 20 mL per hospital cohort patient) was diluted 1:3.3 in PBS, and centrifuged (6,000 *g*, 10 min, 4 °C). The supernatant was loaded on a column containing 3 mL of epoxy-MTBD-tau (prepared with a previous overnight incubation of MTBD-tau and epoxy resin in a binding buffer of 0.1 M NaH_2PO_4–NaOH, 1 M NaCl, pH 9.2) by repetitive loading of the plasma sample overnight at 4 °C. The column was washed with 50 mL of PBS, and MTBD-tau autoantibodies were eluted four times with 5 mL 0.1 M glycine–HCl, pH 2.5, and immediately neutralized to pH 7.0 with 1 M Tris-HCl. Fractions containing antibodies against MTBD-tau were

433 identified using an indirect colorimetric ELISA. Fractions containing the eluted antibodies were
434 stepwise concentrated using Amicon® Ultra-15, Ultra-4, and Ultra-0.5 mL centrifugal filter units
435 (50-kDa MWCO) to up to a volume of 1 mL.

436 **Competitive ELISAs**

437 For the competitive ELISAs of MTBD-tau autoantibodies, high-binding 384-well plates (Perkin
438 Elmer, SpectraPlate 384 HB) were coated with 20 µL of 0.5 µg/mL of MTBD-tau at 4 °C over-
439 night. Afterwards, plates were washed 3x with PBST with a Biotek El406 washer dispenser and
440 blocked with 5% SureBlock™ (Lubio) in PBST for 120 min. Purified autoantibodies from hospital
441 cohort patients' plasma were diluted 1:50 in 1% SureBlock™ (Lubio) in PBST (sample buffer).
442 Anti-tau RD4 mouse monoclonal antibody (05-804 clone 1E1/A6 Merck Millipore) was diluted to
443 a final concentration of 0.4 µg/mL. Bovine serum albumin (Thermo Scientific), in house purified
444 recombinant MTBD-tau, a pool of eight synthetic peptides covering the sequence of MTBD-tau
445 with 25 amino acids length and 10 amino acids of overlap (Genscript) and an unrelated 25 amino
446 acid length synthetic TREM2 (Triggering receptor expressed on myeloid cells 2) peptide
447 (GenScript) were used as competing antigens. Antibody samples were incubated overnight at 4°C
448 with serial 2-fold dilutions of antigens solutions in sample buffer from 20,000 nM to 2.44 nM final
449 concentration. Antibody-antigen solutions were added to the plates and incubated for 45 min at
450 RT. Plates were washed 3x with PBST using a Biotek El406 washer dispenser and secondary
451 antibodies were added as follows: peroxidase AffiniPure® goat anti-Human IgG (H+L) (109-035-
452 088, Jackson ImmunoResearch) diluted 1:3,000 and peroxidase AffiniPure® goat anti-mouse IgG
453 H+L (115-035-003, Jackson ImmunoResearch) diluted 1:2,000. Secondary antibodies were incu-
454 bated for 60 min at RT and then plates were washed plates 4x with PBST. TMB Chromogen So-
455 lution for ELISA (Invitrogen) was added to the plates and incubated for 7 min at RT. Finally, 0.5
456 M H_2SO_4 was added. Plates were briefly centrifuged after each dispensing step except after dis-
457 pensing colorimetric substrate. Plates were read at OD = 450 nm in a plate reader (SpectraMax®
458 Paradigm®, Molecular Devices).

459 For the competitive sandwich ELISAs for the detection of tau in plasma, a similar approach was
460 applied with several changes. High-binding 384-well plates (Perkin Elmer, SpectraPlate 384 HB)
461 were coated with 4 µg/mL BT2 tau monoclonal antibody (epitope on human tau, RSGYS, between
462 residue 194 and 198) (#MN1010, Thermo Fisher) in PBS. Samples were diluted in sample buffer
463 as follows: recombinant human tau^{441} (rPeptide) was diluted to a final concentration of 0.015

ng/mL and incubated with purified anti-tau autoantibodies four-fold serially diluted (1:1.66 to 1:106.6) in 1:2 plasma for 120 min at 37°C with rotation at 500 rpm. Samples were transferred to BT2 antibody-coated plates and incubated for 45 min at RT. Plates were then washed 4x with PBST and ab64193(epitope Ser262 on non-phosphorylated and phosphorylated of human tau) polyclonal IgG antibody (Abcam) at 0.125 µg/mL was incubated for 45 min at RT. Plates were washed 4x with PBST and peroxidase AffiniPure® goat anti-Rabbit IgG (H+L) (111-035-045, Jackson ImmunoResearch) diluted 1:2,000 was incubated 60min at RT. Plates were washed plates 4x with PBST, and 1-Step™ Ultra TMB-ELISA solution (Thermo Fisher) was incubated for 7 min at RT. After addition of 0.5 M H_2SO_4, plates were read at OD = 450 nm in a plate reader (Perkin Elmer, Envision).

Indirect ELISAs

To test for polyreactivity, purified anti-tau autoantibodies were tested by indirect ELISA against several antigens (*50, 51*). High-binding 384-well plates (Perkin Elmer, SpectraPlate 384 HB) were coated with 1 µg/mL of in house purified MTBD-tau in PBS, 10 µg/mL of double stranded DNA from calf-thymus (Sigma) in PBS, 10 µg/mL of lipopolysaccharides from E.*coli* O111:B4 (Sigma) in PBS, 5 µg/mL of human recombinant insulin (Sigma) in PBS, 10 µg/mL of bovine serum albumin (Thermo Fisher) in PBS, 2 µg/mL of cardiolipin solution from bovine heart (Sigma) in ethanol or left high-binding plates uncoated at 4 °C overnight. Plates were washed 3x with PBST using a Biotek El406 washer dispenser and then blocked 5% SureBlock™ (Lubio) in PBST for 120 min at RT. The following samples serially diluted 1:1 in sample buffer were incubated for 120 min at RT: patient purified anti-tau autoantibodies were diluted 1:33, human IgG-depleted plasma (BioSource) was 1:50 diluted and used as a negative control, anti-DNP (Sigma) was diluted to a final concentration of 6 µg/mL and used as a positive control for cardiolipin, DNA and albumin coated plates, anti-tau RD4 mouse monoclonal antibody (05-804 clone 1E1/A6 Merck Millipore) was diluted to a final concentration of 6 µg/mL and used as a positive control for MTBD-tau coated plates, pooled plasma from 20 patients (Institute Clinical Chemistry (IKC), University Hospital Zurich) was diluted 1:25 and used as a positive control for insulin, lipopolysaccharides and uncoated plates. Plates were then washed 4x with PBS-T using a Biotek El406 washer dispenser. Secondary antibodies were diluted and incubated for 60 min at RT as follows: peroxidase AffiniPure® goat anti-human IgG (H+L) (109-035-088, Jackson ImmunoResearch) diluted 1:3,000 and added to purified MTBD-tau autoantibodies and IKC pool wells, peroxidase AffiniPure® goat

anti-mouse IgG H+L (115-035-003, Jackson ImmunoResearch) diluted 1:2,500 and added to anti-RD4 wells, and peroxidase AffiniPure® goat anti-rabbit IgG (H+L) (111-035-045, Jackson ImmunoResearch) diluted 1:4,000 and added to anti-DNP wells. Plates were washed plates 4x with PBST. TMB Chromogen solution for ELISA (Invitrogen) was incubated for 7 min at RT. Finally, 0.5 M H_2SO_4 was added. Plates were briefly centrifuged after each dispensing step except after dispensing colorimetric substrate. Plates were read at OD = 450nm in a plate reader (SpectraMax® Paradigm®, Molecular Devices).

For relative affinity measurements, we used a similar approach with the following modifications. An indirect ELISA in 384-well plates (Perkin Elmer, SpectraPlate 384 HB) with MTBD-tau as a coating antigen, was used. The starting concentration of all antibodies, assayed in triplicates, was 10 µg/mL. They were successively diluted 1:3 to reach a concentration of $2x10^{-6}$ µg/mL. As reference antibody, we used purified RD4 kindly provided by Prof. Rohan de Silva (UCL Queen Square Institute of Neurology, London, UK). As additional controls, we used anti-LAG3 (Lymphocyte Activation Gene 3) antibody Relatlimab (*27*), $\alpha\tau^-$ plasma sample and uncoated plates. The respective EC_{50} values were determined using logistic regression, as described below.

For IgG subclassing, the following secondary antibodies were used: rabbit anti-human IgG1 (SA5-10202, Invitrogen), rabbit anti-human IgG2 (SA5-10203, Invitrogen), rabbit anti-human IgG3 (SA5-10204, Invitrogen) or rabbit anti-human IgG4 (SA5-10205, Invitrogen) diluted 1:1,500, peroxidase AffiniPure® goat anti-rabbit IgG (H+L) antibody (111-035-045, Jackson ImmunoResearch) diluted 1:2,500.

For immunoglobulin light chain typing, the following secondary antibodies were used: peroxidase goat anti-human κ (*22*) 1:4,000 diluted, peroxidase goat anti-human λ (*22*) 1:4,000 diluted.

For epitope mapping, a similar approach was used: high-binding 384-well plates (Perkin Elmer, SpectraPlate 384 HB) with 1 µg/mL of each individual MTBD-tau synthetic peptide (GenScript) diluted in PBS at 4 °C overnight. 8 synthetic peptides spanning the sequence of MTBD-tau with 25 amino acids length and 10 amino acids of overlap were used. Plasma samples were diluted 1:50, human IgG-depleted serum (MyBioSource) was 1:50 diluted and used as a negative control and anti-tau RD4 mouse monoclonal antibody (05-804 clone 1E1/A6 Merck Millipore) was diluted to a final concentration of 6 µg/mL and used as a positive control. The following secondary antibodies diluted in sample buffer were used: peroxidase AffiniPure® goat anti-human IgG (H+L) (109-

035-088, Jackson ImmunoResearch) diluted 1:5,000 and peroxidase AffiniPure® goat anti-mouse IgG H+L (115-035-003, Jackson ImmunoResearch) diluted 1:2,500 and added to anti-RD4 wells.

In vitro MTBD-tau aggregation assay

MTBD-tau *in vitro* aggregation experiments were performed as previously described *(28)*. Briefly, 7 µM of in house purified recombinant MTBD-tau, 3.5 µM of heparin (Santa Cruz Biotechnology) and 10 µM of thioflavin T (ThT, Sigma) were diluted in PBS. The patient purified anti-tau auto-antibodies and controls (plasma sample reactive against the LAG3 and IgG-purified using Protein G Sepharose (Cytiva)) were added at the indicated apparent stoichiometries in Fig. 3A and the mixtures with a total volume of 200 µl were added to black 96-well polystyrene microplates (Nunc, Prod. No. 265301). Measurements of ThT fluorescence (450/480 nm ex/em filters; bottom read mode) were performed at 37°C under continuous orbital shaking (425 cpm) every 15 min for 96 h in a FLUOstar Omega microplate reader (BMG Labtech).

Western blotting

SH-SY5Y wild-type cells (Sigma) and SH-SY5Y cells overexpressing double-mutant tau$^{P301L/S320F}$ were lysed in 0.5% Triton™ X-100 (Sigma Aldrich) in PBS, supplemented with cOmplete™ Mini EDTA-free Protease Inhibitor Cocktail (Roche) on ice and supernatant was recovered after centrifugation (14,000g, 20min, 4°C). Protein concentration was estimated using a bicinchoninic acid assay (Pierce BCA Protein Assay Kit, Thermo Fisher) and sample volumes were adapted to 30 µg of total protein. Samples were loaded onto NuPAGE 12% Bis-Tris gels (Invitrogen). Gels were loaded in the following repeating pattern: protein ladder, SH-SY5Y wt and SH-SY5Y tau$^{P301L/S320F}$ cell lysates. SDS-PAGE gels were run at 180 V in MES buffer for 45 min, transferred to nitrocellulose membranes (Invitrogen) using a dry transfer system (iBlot 2 Gel Transfer Device, Invitrogen, Thermo Fisher), membranes were cut vertically along the protein ladder and blocked with 5% SureBlock (Lubio Science) in PBST for 30 min at RT. Membranes were incubated with patient purified anti-tau autoantibodies 1:100 diluted in in 1% SureBlock in PBST overnight at 4 °C. Negative control membranes were not incubated with primary antibodies. Membranes were washed 3x for 5 min with PBST and then incubated with the following secondary antibodies for 60 min at RT: peroxidase AffiniPure® goat anti-mouse IgG H+L (115-035-003, Jackson ImmunoResearch) 1:10,000 and peroxidase AffiniPure® goat anti-human IgG (H+L) (109-035-088, Jackson ImmunoResearch) 1:10,000 diluted with 1% SureBlock in PBST. The negative control was only incubated with peroxidase goat anti-human secondary antibody. Monoclonal mouse anti-actin clone

C4 (MAB1501R, Chemicon) diluted 1:10,000 in 1% SureBlock in PBST was used as a loading control. Membranes were washed 4x for 5 min with PBST and developed using the Immobilon Crescendo HRP Substrate (Millipore). Individual membranes were imaged using the Fusion SOLO S imaging system (Vilber).

Immunofluorescence studies

SH-SY5Y cells were transiently transfected with EGFP-0N4Rtau, using a Lipofectamine™ 2000 (Invitrogen) according to manufacturer's protocol and a pRK5 plasmid encoding EGFP-0N4RTau (Addgene #46904, kind gift from Dr. Karen Ashe (*52*)), a human four-repeat isoform of tau tagged with enhanced green fluorescent protein (EGFP) at the N-terminus. After 48 h cells were fixed with 4% paraformaldehyde, permeabilized with 0.5% BSA, 0.1% Triton™ X-100 in PBS for 20 min at RT and blocked with 0.5% BSA in PBS for 60 min at RT. Primary antibodies were incubated for 60 min at RT diluted in 0.5% BSA in PBS as follows: purified anti-tau autoantibodies were diluted 1:25, tau mouse monoclonal antibody HT7 (MN1000, Thermo Fisher) diluted 1:500 and used as a positive control. Negative controls were not incubated with primary antibodies. Cells were washed 3x with 0.5% BSA in PBS and incubated 30 min at RT as follows: for HT7 stains with goat anti-mouse IgG (H+L) cross-adsorbed Alexa Fluor ™ 555 (A-21422, Invitrogen) diluted 1:500 and counterstained with 4,6-diamidino-2-phenylindole (DAPI) 1mg/mL (Thermo Fisher) diluted 1:10,000 in 0.5% BSA in PBS, and for purified anti-tau autoantibodies and negative controls with biotin AffiniPure® goat anti-human IgG (H+L) (109-065-003, Jackson ImmunoResearch) diluted 1:200 in 0.5% BSA in PBS. For purified anti-tau autoantibodies and negative controls, cells were further incubated for 30 min at RT with streptavidin Alexa Fluor™ 594 conjugate diluted 1:200 and counterstained with DAPI diluted 1:10,000 in 0.5% BSA in PBS. Before mounting on glass sides, cells were washed cells 2x for 3 min in 0.5% BSA in PBS. Cells were mounted on glass slides with Fluorescence Mounting Medium (Dako) and imaged with a TCS SP5 confocal laser scanning microscope (Leica). Imaging was performed with equipment from the Center for Microscopy and Image Analysis, University of Zurich.

Statistical analysis

Negative logarithm half-maximal response, or "$\log_{10}(EC_{50})$" values, were determined by fitting the OD = 450nm of the eight dilution points of each sample tested in the automated microELISA to a logistic regression fitter (*21*). Samples with a mean squared residual error >20% of the $\log_{10}(EC_{50})$ were classified as non-fittable and were not included in the analysis, as shown before

(*22*). We used -$\log_{10}(EC_{50})$ as a surrogate of antibody titers and classified as positives/ $\alpha\tau^{+}$ the samples with a high -$\log_{10}(EC_{50})$, using a cut-off of -$\log_{10}(EC_{50})$ ≥1.8 for the high-throughput screen. In cases where more than one sample was available for the same individual the most recent $\log_{10}(EC_{50})$ value was used.

Demographic features were available for the hospital cohort as well as the blood donors' cohort. Age is presented as median with interquartile range and comparisons were performed using non-parametric Mann-Whitney U test. Categorized age groups and sex of positive and negative are shown as percentages and compared using two-proportions Z-test or χ^2 test for trend in proportions as indicated. We used log-binomial regression models (*24, 53*) to investigate the association between the detection of anti-MTBD-tau IgG autoantibodies and different demographic features. Risk ratios and 95% confidence intervals were calculated using MTBD-tau autoreactivity as a binomial outcome.

Log-binomial regression models used MTBD-tau-autoreactivity as a binomial outcome and were adjusted for age and sex allowing the estimation of age-and-sex adjusted risk ratios and 95% confidence intervals. For the exploration of the association between MTBD-tau-autoreactivity and neurological disorders, we used multivariate log-binomial regression models to estimate age-and-sex adjusted risk ratios and 95% confidence intervals using 23 major groups of ICD-10 codes (Supplementary Table S2) corresponding to the neurological disorders identified at least once in the positive samples. For the AD cohort ELISA screen, $\log_{10}(EC_{50})$ values were compared using Mann-Whitney U test.

For the exploration of the association between MTBD-tau-autoreactivity and systemic disorders, we used multivariate log-binomial regression models to estimate age-and-sex adjusted risk ratios and 95% confidence intervals using 27 major groups of ICD-10 codes (Supplementary Table S3) or 276 individual ICD-10 codes corresponding to systemic disorders identified at least once in the positive samples and with at least 200 total counts to avoid overinterpretation of rare cases of disease. Individual disease entities with a P value < 0.05 Bonferroni corrected for multiple comparisons were included in a multivariate log-binomial regression analysis. In addition, we conducted a Bayesian logistic regression as described recently (*21, 54-56*), using -$\text{logit}_{10}(EC_{50})$ values as outcome, i.e. without dichotomising the outcome using the R package rstanarm and the following priors (prior=normal[0, 2.5, autoscale=TRUE],prior_intercept = normal[5000, 2.5, autoscale=TRUE)] prior_aux = exponential [1, autoscale =TRUE]. We thereby aimed to confirm the

positive association between ICD-10 codes previously identified using a conventional logistic regression model with high $-\log_{10}(EC_{50})$ values. Each ICD-10 code was analyzed in an independent logistic regression and adjusted for age and sex.

For the exploration of the association between MTBD-tau-autoreactivity and clinical laboratory parameters, we used laboratory parameters with more than 2,000 total counts and calculated median values of the total values available for each patient in case of repetition of the clinical laboratory test. We used multivariate log-binomial regression models to estimate age-and-sex adjusted risk ratios and 95% confidence intervals using 106 clinical laboratory tests.

Throughout the manuscript, statistical significance was defined by 2-tailed P value ≤ 0.05. P values were corrected for multiple comparisons using Bonferroni's method when applicable as described in each Figure/Table.

For IgG subclassing, immunoglobulin light chain typing and epitope mapping experiments, we classified samples to be reactive if the OD_{450} was higher than the average of all negatives OD_{450} + 2x the standard deviation of the OD_{450} of the negatives.

For the MTBD-tau aggregation experiments, the mean baseline fluorescence values were subtracted from the mean fluorescence values at each time point which were then normalized to maximum baseline-subtracted fluorescence values and multiplied by 100 *(57)*.

Statistical analyses and data visualization were performed using R version 4.3.2 and RStudio version 1.4.1106 (*58*).

637 **List of Supplementary Materials:**

638 Table S1, S2 and S3

639 Fig. S1, S2 and S3

640

References

1. Y. Gu, F. Oyama, Y. Ihara, Tau is widely expressed in rat tissues. *J Neurochem* **67**, 1235-1244 (1996).
2. M. Uhlen, L. Fagerberg, B. M. Hallstrom, C. Lindskog, P. Oksvold, A. Mardinoglu, A. Sivertsson, C. Kampf, E. Sjostedt, A. Asplund, I. Olsson, K. Edlund, E. Lundberg, S. Navani, C. A. Szigyarto, J. Odeberg, D. Djureinovic, J. O. Takanen, S. Hober, T. Alm, P. H. Edqvist, H. Berling, H. Tegel, J. Mulder, J. Rockberg, P. Nilsson, J. M. Schwenk, M. Hamsten, K. von Feilitzen, M. Forsberg, L. Persson, F. Johansson, M. Zwahlen, G. von Heijne, J. Nielsen, F. Ponten, Proteomics. Tissue-based map of the human proteome. *Science* **347**, 1260419 (2015).
3. K. S. Kosik, C. L. Joachim, D. J. Selkoe, Microtubule-associated protein tau (tau) is a major antigenic component of paired helical filaments in Alzheimer disease. *Proc Natl Acad Sci U S A* **83**, 4044-4048 (1986).
4. C. L. Joachim, J. H. Morris, K. S. Kosik, D. J. Selkoe, Tau antisera recognize neurofibrillary tangles in a range of neurodegenerative disorders. *Ann Neurol* **22**, 514-520 (1987).
5. B. J. Hanseeuw, R. A. Betensky, H. I. L. Jacobs, A. P. Schultz, J. Sepulcre, J. A. Becker, D. M. O. Cosio, M. Farrell, Y. T. Quiroz, E. C. Mormino, R. F. Buckley, K. V. Papp, R. A. Amariglio, I. Dewachter, A. Ivanoiu, W. Huijbers, T. Hedden, G. A. Marshall, J. P. Chhatwal, D. M. Rentz, R. A. Sperling, K. Johnson, Association of Amyloid and Tau With Cognition in Preclinical Alzheimer Disease: A Longitudinal Study. *JAMA Neurol* **76**, 915-924 (2019).
6. N. Mattsson, H. Zetterberg, S. Janelidze, P. S. Insel, U. Andreasson, E. Stomrud, S. Palmqvist, D. Baker, C. A. Tan Hehir, A. Jeromin, D. Hanlon, L. Song, L. M. Shaw, J. Q. Trojanowski, M. W. Weiner, O. Hansson, K. Blennow, A. Investigators, Plasma tau in Alzheimer disease. *Neurology* **87**, 1827-1835 (2016).
7. S. Janelidze, N. Mattsson, S. Palmqvist, R. Smith, T. G. Beach, G. E. Serrano, X. Chai, N. K. Proctor, U. Eichenlaub, H. Zetterberg, K. Blennow, E. M. Reiman, E. Stomrud, J. L. Dage, O. Hansson, Plasma P-tau181 in Alzheimer's disease: relationship to other biomarkers, differential diagnosis, neuropathology and longitudinal progression to Alzheimer's dementia. *Nat Med* **26**, 379-386 (2020).
8. M. M. Mielke, C. E. Hagen, A. M. V. Wennberg, D. C. Airey, R. Savica, D. S. Knopman, M. M. Machulda, R. O. Roberts, C. R. Jack, R. C. Petersen, J. L. Dage, Association of Plasma Total Tau Level With Cognitive Decline and Risk of Mild Cognitive Impairment or Dementia in the Mayo Clinic Study on Aging. *JAMA Neurol* **74**, 1073-1080 (2017).
9. S. Palmqvist, P. Tideman, N. Mattsson-Carlgren, S. E. Schindler, R. Smith, R. Ossenkoppele, S. Calling, T. West, M. Monane, P. B. Verghese, J. B. Braunstein, K. Blennow, S. Janelidze, E. Stomrud, G. Salvado, O. Hansson, Blood Biomarkers to Detect Alzheimer Disease in Primary Care and Secondary Care. *JAMA*, (2024).
10. A. A. Asuni, A. Boutajangout, D. Quartermain, E. M. Sigurdsson, Immunotherapy targeting pathological tau conformers in a tangle mouse model reduces brain pathology with associated functional improvements. *J Neurosci* **27**, 9115-9129 (2007).
11. A. Boutajangout, J. Ingadottir, P. Davies, E. M. Sigurdsson, Passive immunization targeting pathological phospho-tau protein in a mouse model reduces functional decline and clears tau aggregates from the brain. *J Neurochem* **118**, 658-667 (2011).

12. E. E. Congdon, E. M. Sigurdsson, Tau-targeting therapies for Alzheimer disease. *Nat Rev Neurol* **14**, 399-415 (2018).
13. T. L. Rothstein, Natural Antibodies as Rheostats for Susceptibility to Chronic Diseases in the Aged. *Front Immunol* **7**, 127 (2016).
14. H. U. Lutz, C. J. Binder, S. Kaveri, Naturally occurring auto-antibodies in homeostasis and disease. *Trends Immunol* **30**, 43-51 (2009).
15. J. R. Jaycox, Y. Dai, A. M. Ring, Decoding the autoantibody reactome. *Science* **383**, 705-707 (2024).
16. N. R. Florance, R. L. Davis, C. Lam, C. Szperka, L. Zhou, S. Ahmad, C. J. Campen, H. Moss, N. Peter, A. J. Gleichman, C. A. Glaser, D. R. Lynch, M. R. Rosenfeld, J. Dalmau, Anti-N-methyl-D-aspartate receptor (NMDAR) encephalitis in children and adolescents. *Ann Neurol* **66**, 11-18 (2009).
17. V. A. Lennon, D. M. Wingerchuk, T. J. Kryzer, S. J. Pittock, C. F. Lucchinetti, K. Fujihara, I. Nakashima, B. G. Weinshenker, A serum autoantibody marker of neuromyelitis optica: distinction from multiple sclerosis. *Lancet* **364**, 2106-2112 (2004).
18. J. Ferrero, L. Williams, H. Stella, K. Leitermann, A. Mikulskis, J. O'Gorman, J. Sevigny, First-in-human, double-blind, placebo-controlled, single-dose escalation study of aducanumab (BIIB037) in mild-to-moderate Alzheimer's disease. *Alzheimers Dement (N Y)* **2**, 169-176 (2016).
19. A. Bartos, L. Fialová, J. Švarcová, Lower Serum Antibodies Against Tau Protein and Heavy Neurofilament in Alzheimer's Disease. *J Alzheimers Dis* **64**, 751-760 (2018).
20. Y. Kronimus, A. Albus, M. Balzer-Geldsetzer, S. Straub, E. Semler, M. Otto, J. Klotsche, R. Dodel, L. Consortium, D. Mengel, Naturally Occurring Autoantibodies against Tau Protein Are Reduced in Parkinson's Disease Dementia. *PLoS One* **11**, e0164953 (2016).
21. M. Emmenegger, E. De Cecco, D. Lamparter, R. P. B. Jacquat, J. Riou, D. Menges, T. Ballouz, D. Ebner, M. M. Schneider, I. C. Morales, B. Dogancay, J. Guo, A. Wiedmer, J. Domange, M. Imeri, R. Moos, C. Zografou, L. Batkitar, L. Madrigal, D. Schneider, C. Trevisan, A. Gonzalez-Guerra, A. Carrella, I. L. Dubach, C. K. Xu, G. Meisl, V. Kosmoliaptsis, T. Malinauskas, N. Burgess-Brown, R. Owens, S. Hatch, J. Mongkolsapaya, G. R. Screaton, K. Schubert, J. D. Huck, F. Liu, F. Pojer, K. Lau, D. Hacker, E. Probst-Muller, C. Cervia, J. Nilsson, O. Boyman, L. Saleh, K. Spanaus, A. von Eckardstein, D. J. Schaer, N. Ban, C. J. Tsai, J. Marino, G. F. X. Schertler, N. Ebert, V. Thiel, J. Gottschalk, B. M. Frey, R. R. Reimann, S. Hornemann, A. M. Ring, T. P. J. Knowles, M. A. Puhan, C. L. Althaus, I. Xenarios, D. I. Stuart, A. Aguzzi, Continuous population-level monitoring of SARS-CoV-2 seroprevalence in a large European metropolitan region. *iScience* **26**, 105928 (2023).
22. A. Senatore, K. Frontzek, M. Emmenegger, A. Chincisan, M. Losa, R. Reimann, G. Horny, J. Guo, S. Fels, S. Sorce, C. Zhu, N. George, S. Ewert, T. Pietzonka, S. Hornemann, A. Aguzzi, Protective anti-prion antibodies in human immunoglobulin repertoires. *EMBO Mol Med* **12**, e12739 (2020).
23. M. Emmenegger, C. Zografou, D. Yile, L. R. Hoyt, R. Gudneppanavar, A. Chincisan, H. Rehrauer, F. J. Noé, N. Zajac, G. Meisl, M. M. Schneider, H. Nguyen, K. Höpker, T. P. J. Knowles, M. Sospedra, R. Martin, A. M. Ring, S. Leeds, S. C. Eisenbarth, M. E. Egan, E. M. Bruscia, A. Aguzzi, The Cystic Fibrosis Transmembrane Regulator Controls Tolerogenic Responses to Food Allergens in Mice and Humans. *medRxiv*, (2024).

24. F. A. Diaz-Quijano, A simple method for estimating relative risk using logistic regression. *BMC Med Res Methodol* **12**, 14 (2012).
25. M. W. Donoghoe, I. C. Marschner, Logbin: An R Package for Relative Risk Regression Using the Log-Binomial Model. *Journal of Statistical Software* **86**, (2018).
26. R. de Silva, T. Lashley, G. Gibb, D. Hanger, A. Hope, A. Reid, R. Bandopadhyay, M. Utton, C. Strand, T. Jowett, N. Khan, B. Anderton, N. Wood, J. Holton, T. Revesz, A. Lees, Pathological inclusion bodies in tauopathies contain distinct complements of tau with three or four microtubule-binding repeat domains as demonstrated by new specific monoclonal antibodies. *Neuropathol Appl Neurobiol* **29**, 288-302 (2003).
27. M. Emmenegger, E. De Cecco, M. Hruska-Plochan, T. Eninger, M. M. Schneider, M. Barth, E. Tantardini, P. de Rossi, M. Bacioglu, R. G. Langston, A. Kaganovich, N. Bengoa-Vergniory, A. Gonzalez-Guerra, M. Avar, D. Heinzer, R. Reimann, L. M. Hasler, T. W. Herling, N. S. Matharu, N. Landeck, K. Luk, R. Melki, P. J. Kahle, S. Hornemann, T. P. J. Knowles, M. R. Cookson, M. Polymenidou, M. Jucker, A. Aguzzi, LAG3 is not expressed in human and murine neurons and does not modulate alpha-synucleinopathies. *EMBO Mol Med* **13**, e14745 (2021).
28. A. Apetri, R. Crespo, J. Juraszek, G. Pascual, R. Janson, X. Zhu, H. Zhang, E. Keogh, T. Holland, J. Wadia, H. Verveen, B. Siregar, M. Mrosek, R. Taggenbrock, J. Ameijde, H. Inganäs, M. van Winsen, M. H. Koldijk, D. Zuijdgeest, M. Borgers, K. Dockx, E. J. M. Stoop, W. Yu, E. C. Brinkman-van der Linden, K. Ummenthum, K. van Kolen, M. Mercken, S. Steinbacher, D. de Marco, J. J. Hoozemans, I. A. Wilson, W. Koudstaal, J. Goudsmit, A common antigenic motif recognized by naturally occurring human V. *Acta Neuropathol Commun* **6**, 43 (2018).
29. M. P. Pase, A. S. Beiser, J. J. Himali, C. L. Satizabal, H. J. Aparicio, C. DeCarli, G. Chêne, C. Dufouil, S. Seshadri, Assessment of Plasma Total Tau Level as a Predictive Biomarker for Dementia and Related Endophenotypes. *JAMA Neurol* **76**, 598-606 (2019).
30. E. Barini, G. Plotzky, Y. Mordashova, J. Hoppe, E. Rodriguez-Correa, S. Julier, F. LePrieult, I. Mairhofer, M. Mezler, S. Biesinger, M. Cik, M. W. Meinhardt, E. Ercan-Herbst, D. E. Ehrnhoefer, A. Striebinger, K. Bodie, C. Klein, L. Gasparini, K. Schlegel, Tau in the brain interstitial fluid is fragmented and seeding-competent. *Neurobiol Aging* **109**, 64-77 (2022).
31. M. W. Donoghoe, I. C. Marschner, logbin: An R Package for Relative Risk Regression Using the Log-Binomial Model. *Journal of Statistical Software* **86**, 21 (2018).
32. L. Dahm, C. Ott, J. Steiner, B. Stepniak, B. Teegen, S. Saschenbrecker, C. Hammer, K. Borowski, M. Begemann, S. Lemke, K. Rentzsch, C. Probst, H. Martens, J. Wienands, G. Spalletta, K. Weissenborn, W. Stöcker, H. Ehrenreich, Seroprevalence of autoantibodies against brain antigens in health and disease. *Ann Neurol* **76**, 82-94 (2014).
33. Z. Y. Yu, W. W. Li, H. M. Yang, N. B. Manucat-Tan, J. Wang, Y. R. Wang, B. L. Sun, Z. C. Hu, L. L. Zhang, L. Tan, J. Deng, Y. H. Liu, Naturally Occurring Antibodies to Tau Exists in Human Blood and Are Not Changed in Alzheimer's Disease. *Neurotox Res* **37**, 1029-1035 (2020).
34. Y. Tsuboi, R. J. Uitti, M. B. Delisle, J. J. Ferreira, C. Brefel-Courbon, O. Rascol, B. Ghetti, J. R. Murrell, M. Hutton, M. Baker, Z. K. Wszolek, Clinical features and disease haplotypes of individuals with the N279K tau gene mutation: a comparison of the pallidopontonigral degeneration kindred and a French family. *Arch Neurol* **59**, 943-950 (2002).

35. I. Sotiropoulos, M. C. Galas, J. M. Silva, E. Skoulakis, S. Wegmann, M. B. Maina, D. Blum, C. L. Sayas, E. M. Mandelkow, E. Mandelkow, M. G. Spillantini, N. Sousa, J. Avila, M. Medina, A. Mudher, L. Buee, Atypical, non-standard functions of the microtubule associated Tau protein. *Acta Neuropathol Commun* **5**, 91 (2017).
36. M. M. Rinschen, M. Gödel, F. Grahammer, S. Zschiedrich, M. Helmstädter, O. Kretz, M. Zarei, D. A. Braun, S. Dittrich, C. Pahmeyer, P. Schroder, C. Teetzen, H. Gee, G. Daouk, M. Pohl, E. Kuhn, B. Schermer, V. Küttner, M. Boerries, H. Busch, M. Schiffer, C. Bergmann, M. Krüger, F. Hildebrandt, J. Dengjel, T. Benzing, T. B. Huber, A Multi-layered Quantitative In Vivo Expression Atlas of the Podocyte Unravels Kidney Disease Candidate Genes. *Cell Rep* **23**, 2495-2508 (2018).
37. K. H. Ho, X. Yang, A. B. Osipovich, O. Cabrera, M. L. Hayashi, M. A. Magnuson, G. Gu, I. Kaverina, Glucose Regulates Microtubule Disassembly and the Dose of Insulin Secretion via Tau Phosphorylation. *Diabetes* **69**, 1936-1947 (2020).
38. L. Vallés-Saiz, R. Peinado-Cahuchola, J. Ávila, F. Hernández, Microtubule-associated protein tau in murine kidney: role in podocyte architecture. *Cell Mol Life Sci* **79**, 97 (2022).
39. E. E. Congdon, C. Ji, A. M. Tetlow, Y. Jiang, E. M. Sigurdsson, Tau-targeting therapies for Alzheimer disease: current status and future directions. *Nat Rev Neurol* **19**, 715-736 (2023).
40. *ClinicalTrial.gov, NCT05269394, Dominantly Inherited Alzheimer Network Trial: An Opportunity to Prevent Dementia. A Study of Potential Disease Modifying Treatments in Individuals With a Type of Early Onset Alzheimer's Disease Caused by a Genetic Mutation (DIAN-TU),* *(https://clinicaltrials.gov/study/NCT05269394?cond=Alzheimer%20Disease&term=E2814&rank=1)* (2023).
41. M. E. Barton, B. Van Den Steen, H. L. G. Van Tricht, W. Byrnes, F. E. Purcell, S. A. Southcott, D. Raby, Y. I. Starshinov, C. Ewen, Update on the TOGETHER study: a patient- and investigator-blind, randomized, placebo-controlled study evaluating the efficacy, safety and tolerability of bepranemab, UCB0107, in prodromal-to-mild Alzheimer's disease. *Alzheimer's & Dementia* **18**, e068973 (2022).
42. A. Moscoso, M. J. Grothe, N. J. Ashton, T. K. Karikari, J. Lantero Rodríguez, A. Snellman, M. Suárez-Calvet, K. Blennow, H. Zetterberg, M. Schöll, A. s. D. N. Initiative, Longitudinal Associations of Blood Phosphorylated Tau181 and Neurofilament Light Chain With Neurodegeneration in Alzheimer Disease. *JAMA Neurol* **78**, 396-406 (2021).
43. N. R. Barthélemy, Y. Li, N. Joseph-Mathurin, B. A. Gordon, J. Hassenstab, T. L. S. Benzinger, V. Buckles, A. M. Fagan, R. J. Perrin, A. M. Goate, J. C. Morris, C. M. Karch, C. Xiong, R. Allegri, P. C. Mendez, S. B. Berman, T. Ikeuchi, H. Mori, H. Shimada, M. Shoji, K. Suzuki, J. Noble, M. Farlow, J. Chhatwal, N. R. Graff-Radford, S. Salloway, P. R. Schofield, C. L. Masters, R. N. Martins, A. O'Connor, N. C. Fox, J. Levin, M. Jucker, A. Gabelle, S. Lehmann, C. Sato, R. J. Bateman, E. McDade, D. I. A. Network, A soluble phosphorylated tau signature links tau, amyloid and the evolution of stages of dominantly inherited Alzheimer's disease. *Nat Med* **26**, 398-407 (2020).
44. T. K. Karikari, T. A. Pascoal, N. J. Ashton, S. Janelidze, A. L. Benedet, J. L. Rodriguez, M. Chamoun, M. Savard, M. S. Kang, J. Therriault, M. Schöll, G. Massarweh, J. P. Soucy, K. Höglund, G. Brinkmalm, N. Mattsson, S. Palmqvist, S. Gauthier, E. Stomrud, H. Zetterberg,

O. Hansson, P. Rosa-Neto, K. Blennow, Blood phosphorylated tau 181 as a biomarker for Alzheimer's disease: a diagnostic performance and prediction modelling study using data from four prospective cohorts. *Lancet Neurol* **19**, 422-433 (2020).

45. J. C. Park, S. H. Han, D. Yi, M. S. Byun, J. H. Lee, S. Jang, K. Ko, S. Y. Jeon, Y. S. Lee, Y. K. Kim, D. Y. Lee, I. Mook-Jung, Plasma tau/amyloid-β1-42 ratio predicts brain tau deposition and neurodegeneration in Alzheimer's disease. *Brain* **142**, 771-786 (2019).
46. S. Palmqvist, S. Janelidze, Y. T. Quiroz, H. Zetterberg, F. Lopera, E. Stomrud, Y. Su, Y. Chen, G. E. Serrano, A. Leuzy, N. Mattsson-Carlgren, O. Strandberg, R. Smith, A. Villegas, D. Sepulveda-Falla, X. Chai, N. K. Proctor, T. G. Beach, K. Blennow, J. L. Dage, E. M. Reiman, O. Hansson, Discriminative Accuracy of Plasma Phospho-tau217 for Alzheimer Disease vs Other Neurodegenerative Disorders. *JAMA* **324**, 772-781 (2020).
47. K. Yanamandra, T. K. Patel, H. Jiang, S. Schindler, J. D. Ulrich, A. L. Boxer, B. L. Miller, D. R. Kerwin, G. Gallardo, F. Stewart, M. B. Finn, N. J. Cairns, P. B. Verghese, I. Fogelman, T. West, J. Braunstein, G. Robinson, J. Keyser, J. Roh, S. S. Knapik, Y. Hu, D. M. Holtzman, Anti-tau antibody administration increases plasma tau in transgenic mice and patients with tauopathy. *Sci Transl Med* **9**, (2017).
48. M. M. Mielke, J. L. Dage, R. D. Frank, A. Algeciras-Schimnich, D. S. Knopman, V. J. Lowe, G. Bu, P. Vemuri, J. Graff-Radford, C. R. Jack, Jr., R. C. Petersen, Performance of plasma phosphorylated tau 181 and 217 in the community. *Nat Med* **28**, 1398-1405 (2022).
49. C. M. Hedgepeth, L. J. Conrad, J. Zhang, H. C. Huang, V. M. Lee, P. S. Klein, Activation of the Wnt signaling pathway: a molecular mechanism for lithium action. *Dev Biol* **185**, 82-91 (1997).
50. J. J. Bunker, S. A. Erickson, T. M. Flynn, C. Henry, J. C. Koval, M. Meisel, B. Jabri, D. A. Antonopoulos, P. C. Wilson, A. Bendelac, Natural polyreactive IgA antibodies coat the intestinal microbiota. *Science* **358**, (2017).
51. H. Mouquet, J. F. Scheid, M. J. Zoller, M. Krogsgaard, R. G. Ott, S. Shukair, M. N. Artyomov, J. Pietzsch, M. Connors, F. Pereyra, B. D. Walker, D. D. Ho, P. C. Wilson, M. S. Seaman, H. N. Eisen, A. K. Chakraborty, T. J. Hope, J. V. Ravetch, H. Wardemann, M. C. Nussenzweig, Polyreactivity increases the apparent affinity of anti-HIV antibodies by heteroligation. *Nature* **467**, 591-595 (2010).
52. B. R. Hoover, M. N. Reed, J. Su, R. D. Penrod, L. A. Kotilinek, M. K. Grant, R. Pitstick, G. A. Carlson, L. M. Lanier, L. L. Yuan, K. H. Ashe, D. Liao, Tau mislocalization to dendritic spines mediates synaptic dysfunction independently of neurodegeneration. *Neuron* **68**, 1067-1081 (2010).
53. L. A. McNutt, C. Wu, X. Xue, J. P. Hafner, Estimating the relative risk in cohort studies and clinical trials of common outcomes. *Am J Epidemiol* **157**, 940-943 (2003).
54. M. Emmenegger, V. Emmenegger, S. M. Shambat, T. C. Scheier, A. Gomez-Mejia, C. C. Chang, P. D. Wendel-Garcia, P. K. Buehler, T. Buettner, D. Roggenbuck, S. D. Brugger, K. B. M. Frauenknecht, Antiphospholipid antibodies are enriched post-acute COVID-19 but do not modulate the thrombotic risk. *Clin Immunol* **257**, 109845 (2023).
55. M. Emmenegger, V. Emmenegger, in *Zenodo, https://doi.org/10.5281/zenodo.10051979.* (2023).
56. M. Losa, M. Emmenegger, P. De Rossi, P. M. Schürch, T. Serdiuk, N. Pengo, D. Capron, D. Bieli, N. J. Rupp, M. C. Carta, K. J. Karl J Frontzek, V. Lysenko, R. R. Reimann, A. K. K.

Lakkaraju, M. Nuvolone, G. T. Westermark, K. P. R. Nilsson, M. Polymenidou, A. P. A. Theocharides, Simone Hornemann, P. Picotti, A. Aguzzi, The ASC inflammasome adapter controls the extent of peripheral protein aggregate deposition in inflammation-associated amyloidosis. *BioXriv, doi: https://doi.org/10.1101/2021.05.01.442282*, (2023).

57. C. D. Orrú, J. Yuan, B. S. Appleby, B. Li, Y. Li, D. Winner, Z. Wang, Y. A. Zhan, M. Rodgers, J. Rarick, R. E. Wyza, T. Joshi, G. X. Wang, M. L. Cohen, S. Zhang, B. R. Groveman, R. B. Petersen, J. W. Ironside, M. E. Quiñones-Mateu, J. G. Safar, Q. Kong, B. Caughey, W. Q. Zou, Prion seeding activity and infectivity in skin samples from patients with sporadic Creutzfeldt-Jakob disease. *Sci Transl Med* **9**, (2017).

58. RStudioTeam. (RStudio, PBC, Boston, MA, 2021).

Acknowledgments:

The authors wish to thank the hospital patients and blood donors for their generous altruistic contributions to this study. Imaging was performed with equipment maintained by the Center for Microscopy and Image Analysis, University of Zurich. We thank Prof. Rohan de Silva (UCL Queen Square Institute of Neurology, London, UK) for providing the purified anti-MTBD-tau antibody RD4. We thank Dr. Marco Losa for the generous provision of secondary antibodies for light chain typing and Magdalena Bialkowska, Lisa Caflisch, Berre Doğançay, Julie Domange, Marigona Imeri, Lorène Mottier, Rea Müller, Antonella Rosati, Dezirae Schneider, and Anne Wiedmer for help with the high-throughput assays. Insightful advice about programming in R software was provided by Reto Guadagnini.

Funding:

University of Zürich, Candoc grant FK-19-025 (ADM)

Swiss Personalised Health Network, SPHN, driver project grant 2017DRI17 (AA)

Swiss National Foundation SNF (SNSF grant ID 179040 and grant ID 207872, Sinergia grant ID 183563) (AA)

European Research Council ERC Prion2020, 670958 (AA)

Nomis Foundation (AA)

Innovation Fund of the University Hospital Zurich (INOV00096) (AA)

University Hospital Zurich Foundation grant USZF27101 (with contributions of the NOMIS Foundation, the Schwyzer Winiker Stiftung, and the Baugarten Stiftung, AA, ME)

HMZ ImmunoTarget grant, Stiftung Neuropath and GELU Foundation (AA)

Michael J. Fox Foundation (grant ID MJFF-020710 and MJFF-021073) (SH).

Author contributions:

Conceived and designed the experiments: ADM, SH, AA. Supervised the study: SH, AA. Performed tau protein purification: ADM, EDC, JG. Performed tau microELISA automated screen: ADM, ME. Performed amyloid-ß pyroglutamate and cellular prion protein microELISA automated screen: MC, KF, ME. Maintained microELISA automated platform: ME. Performed purification, validation and characterization of anti-tau autoantibodies: ADM, JG. Maintained the clinical database: ME, AC. Performed data analysis and visualization: ADM. Wrote the first draft of manuscript: ADM. Corrected and advised on subsequent versions of the manuscript: ADM, ME, SH, AA. All authors reviewed and approved the final version of the manuscript and consented to be accountable for the work.

Competing interests:

ADM has received a research grant from University of Zurich; KF has received research grants from Ono Pharmaceuticals and Theodor Ida Herzog Egli Stiftung, consulting fees from Acumen Collective and Ionis Pharmaceuticals, support for attending meetings/travel from Euro-CNS and has participated on the Advisory Board of Mabylon AG; AA has received research grants from the Swiss Personalized Health Network, Swiss National Foundation, European Research Council and Nomis Foundation and is a member of the Board of Directors of Mabylon AG. Mabylon AG produces therapeutic human antibodies. Mabylon AG had no insight and no influence on the current study. All authors report no other relationships or activities that could appear to have influenced the submitted work.

Data and materials availability:

Data and material requests should be addressed to the corresponding authors. Materials will be shared upon reasonable request, given the approval by an ethics committee or review board and a material transfer agreement.

921 **Figures**

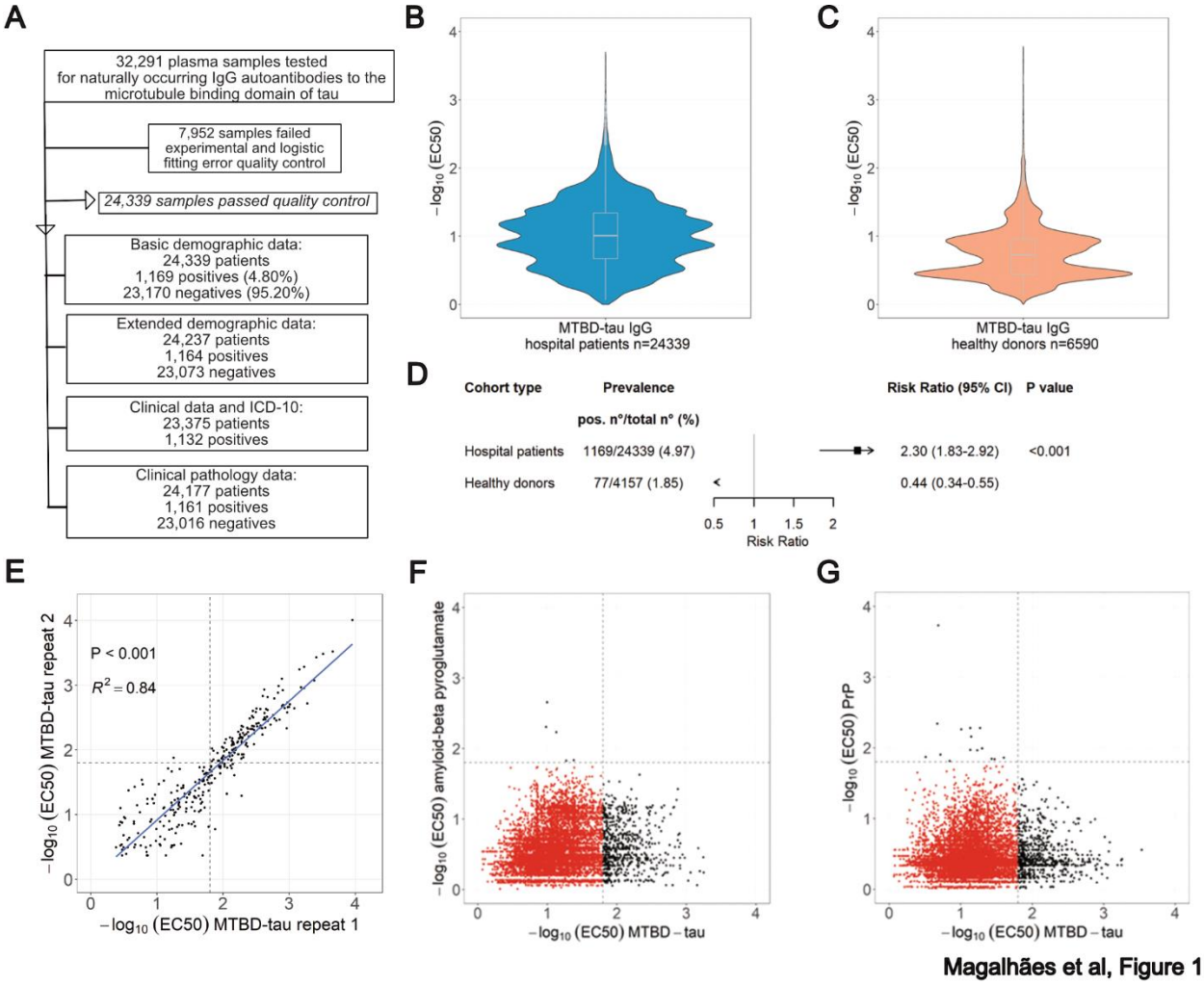

922

923

924 **Fig. 1. Study overview and seroprevalence of anti-MTBD-tau IgG autoantibodies. A.**
925 Flowchart of the study design. **B.-C.** Distribution of -$\log_{10}(EC_{50})$ values obtained from the micro-
926 ELISA screen of hospital (B) and blood donor (C) plasma samples. **D.** Age- and sex-adjusted risk
927 ratio ratios and 95% confidence intervals (CI; I bars) for the detection of anti-tau autoantibodies
928 in hospital and blood-bank plasma samples. **E.** Replicability of microELISA duplicates with inde-
929 pendent estimation of the -$\log_{10}(EC_{50})$ values. Dashed lines: cut-off value of -$\log_{10}(EC_{50})$ = 1.8. **F.**
930 -$\log_{10}(EC_{50})$ values of samples tested by microELISA against MTBD-tau and amyloid-ß pyroglu-
931 tamate. **G.** Same as shown in (F), but for samples tested against MTBD-tau and the cellular prion
932 protein (PrP^{C}).

933

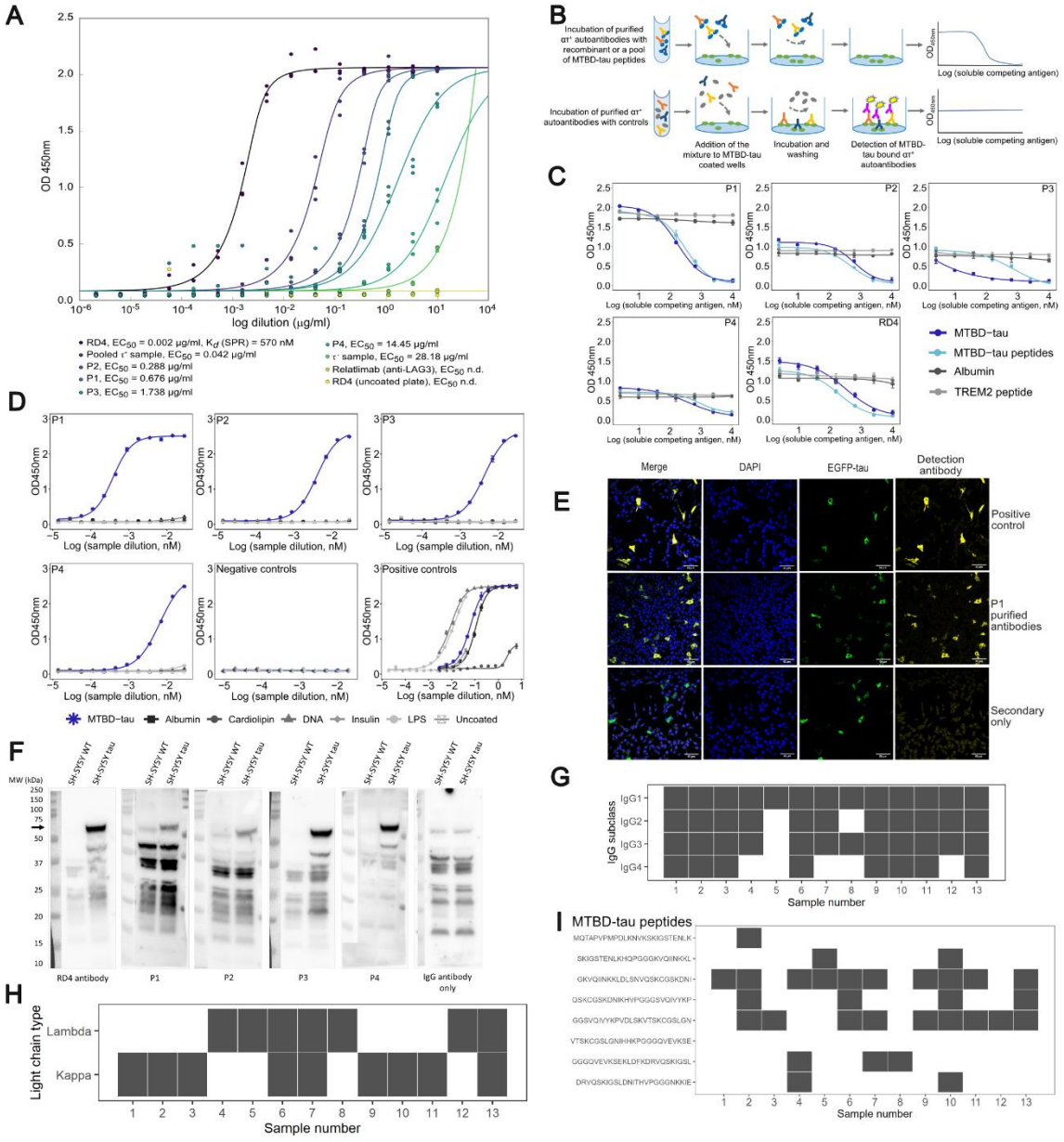

934 Magalhães et al, Figure 2

935 **Fig. 2. Biophysical characterization of samples from ατ$^+$ patients. A**. Indirect ELISA of puri-
936 fied anti-MTBD-tau autoantibodies from four ατ$^+$ samples and from 6 pooled ατ$^+$ samples. All
937 antibodies were assayed at the same concentration to compare their EC_{50} to that of RD4. EC_{50}
938 values are indicated in the Figure. n.d.: not determined. **B.** Principle of competition ELISA. **C.**
939 Competition ELISA of purified anti-tau autoantibodies from four ατ$^+$ patients against albumin,
940 recombinant MTBD-tau, synthetic peptides spanning the sequence of MTBD-tau and synthetic
941 TREM2 RD4 (anti-4-repeat-isoform) antibody: positive control. Mean values ± SD of two repli-

cates. **D.** Indirect ELISA to assess the reactivity of purified anti-tau autoantibodies against albumin, cardiolipin, double-stranded DNA, insulin, lipopolysaccharides (LPS), MTBD-tau and uncoated plates. Positive controls were as follows: RD4 antibody for MTBD-tau, anti-DNP antibody for cardiolipin, albumin and DNA and the IKC pool of 20 heparin plasma samples for insulin, LPS and uncoated plates. Mean values ± SD of two replicates are shown. **E.** Representative immunofluorescence images of SH-SY5Y cells expressing EGFP-0N4R-tau using affinity-purified anti-tau autoantibodies. HT7 pan-tau antibody: positive control. No primary antibody: negative control. Scale bar: 60 µm. **F.** Western blot of cell lysates from wild-type (SH-SY5Y WT) or tau$^{P301L/S320F}$-overexpressing cells (SH-SY5Y tau) using purified anti-tau autoantibodies from four $\alpha\tau^{+}$ patients. Positive control: RD4. Negative control: omission of primary antibody. **G.** IgG subclass typing of 13 $\alpha\tau^{+}$ plasma samples. Gray and white boxes: reactive and non-reactive samples, respectively. **H.** κ/λ light chain typing of the samples in F. **I.** Epitope mapping of the samples in Fig. 2F against 25mer MTBD-tau peptides with 10 residues overlap. Vertical axis: sequences of the MTBD-tau peptides covering the sequence of MTBD-tau.

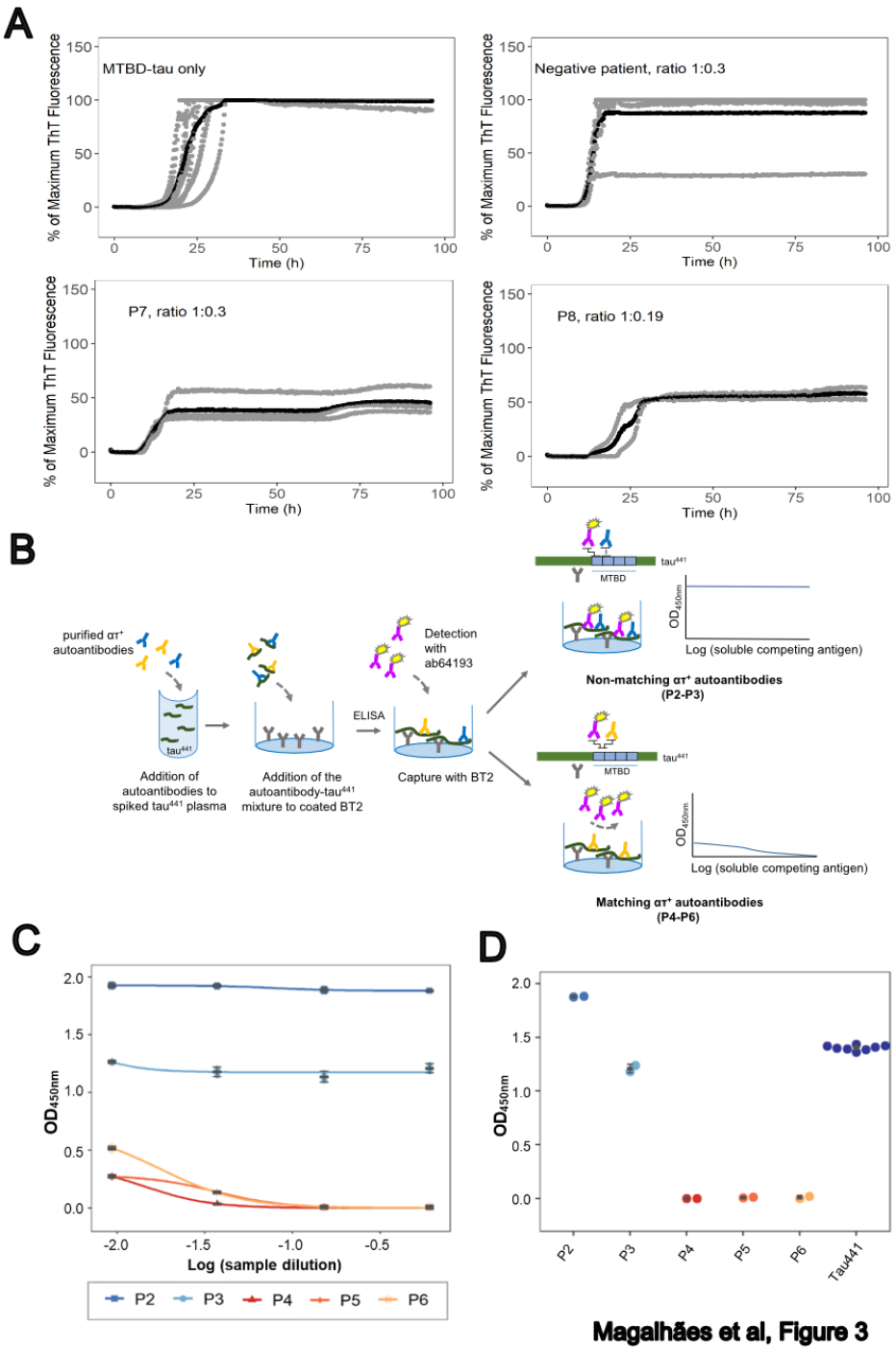

Fig. 3. Natural ατ autoantibodies inhibit tau aggregation and impair tau detection. A. Kinetic aggregation curves of MTBD-tau followed by ThT fluorescence in the absence (n=12) or presence of purified ατ autoantibodies (patient P7 (n=4) and P8 (n=2)) or antibodies from an $\alpha\tau^-$ sample (n=6). Stoichiometric ratios as indicated. Gray lines indicate individual replicates and black lines the average of the replicates. **B.** Principle of the competition sandwich ELISA. **C.** Competitive

962 sandwich ELISA to assess the ability of purified anti-tau autoantibodies with matching (P4-P6)
963 and non-matching (P2 and P3) epitopes to the commercial detection antibody, ab64193, to impair
964 the detection of free tau^{441} spiked in plasma (dark blue). Serial dilutions of purified anti-tau anti-
965 bodies are shown in (C) and binding at highest anti-tau antibody concentrations in (D).
966

967

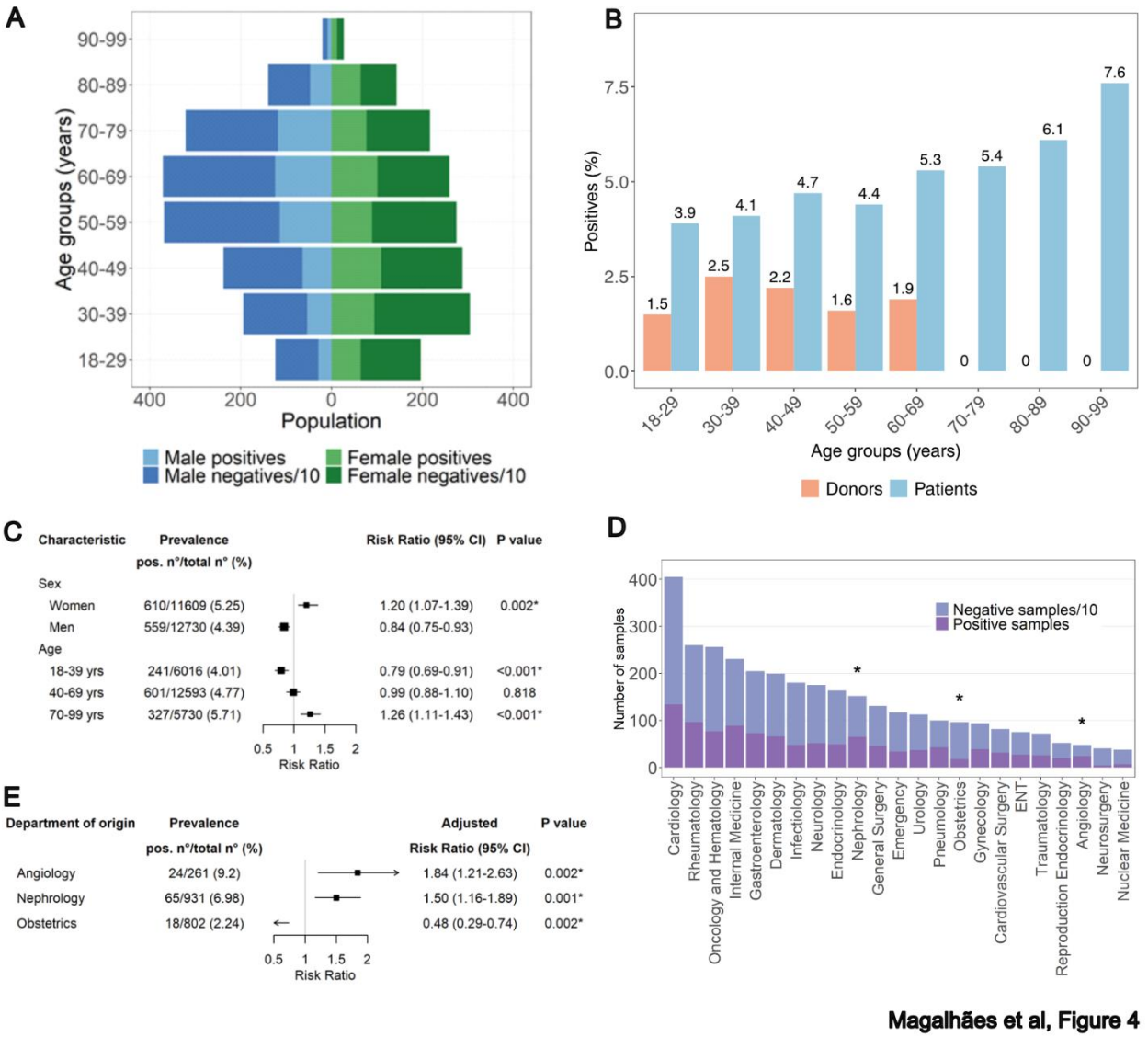

968

969 **Fig. 4. Demographic characteristics of hospital patients' cohort. A.** Age and sex pyramid of
970 positive and negative individuals. **B.** Percentage of positives across decadic age groups. The num-
971 bers on top of each bar correspond to the positivity rates. Numbers inside bars: $\alpha\tau^+$ vs tested sam-
972 ples in each age group. χ^2 test for trend in proportions. **C.** Risk ratios ± 95% confidence intervals
973 (CI) for $\alpha\tau^+$ autoantibodies according to sex and age groups. Asterisks: $P < 0.05$ after Bonferroni
974 correction. **D.** Break-down of samples by clinical department. Asterisks: $P < 0.05$ (two-proportions
975 z-test with Bonferroni correction). **E.** Age- and sex-adjusted risk ratios ± 95% CI for $\alpha\tau^+$ samples
976 by clinical department. Asterisks: $P < 0.05$ after Bonferroni correction.

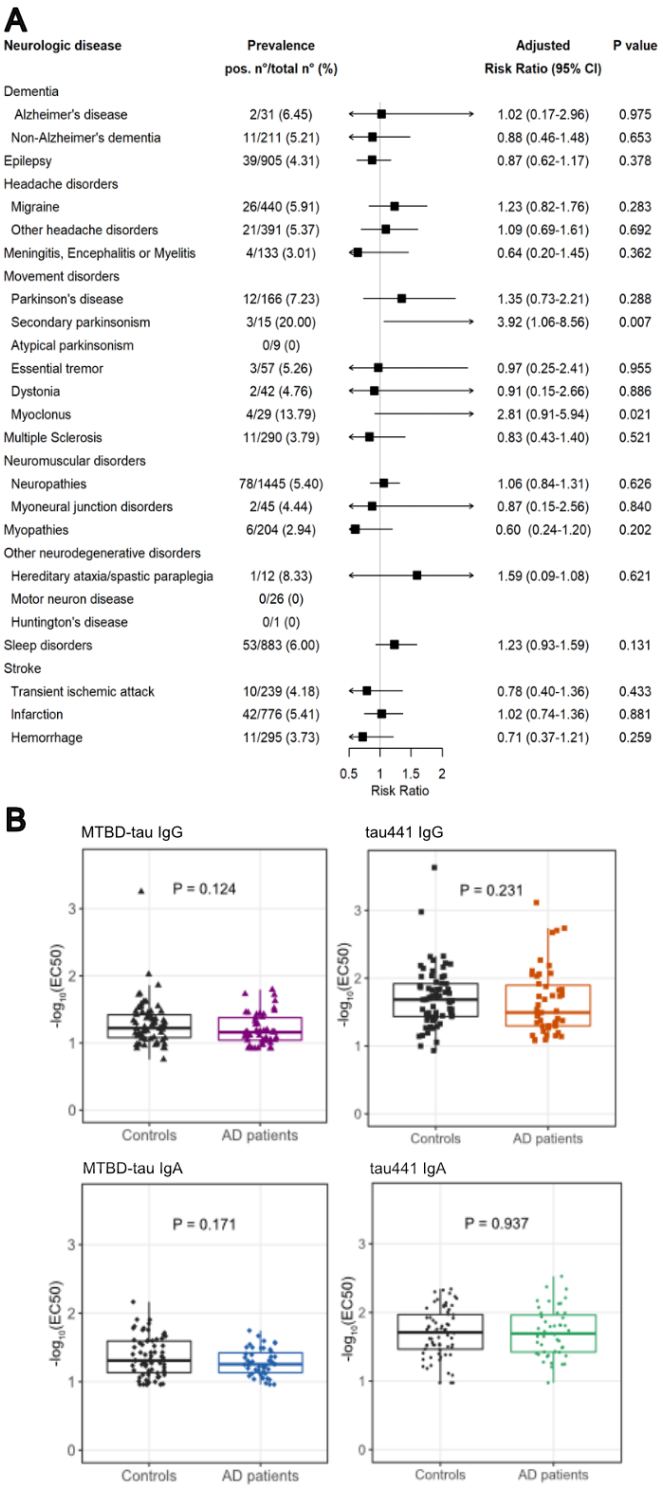

977 **Magalhães et al, Figure 5**

978 **Fig. 5. Age- and sex-adjusted risk ratios of MTBD-tau-autoreactivity for major groups of**
979 **neurological disorders and reactivity profiles for AD screen**. **A.** Age- and sex-adjusted risk
980 ratios and 95% confidence intervals (CI; I bars) for $\alpha\tau^{+}$ autoantibodies according to different

groups of neurological disorders. No P values remained significant after Bonferroni correction. **B.** Boxplots showing the 25^{th}, 50^{th} (median) and 75^{th} percentiles of the reactivity profiles for AD and control patients (Mann-Whitney U test).

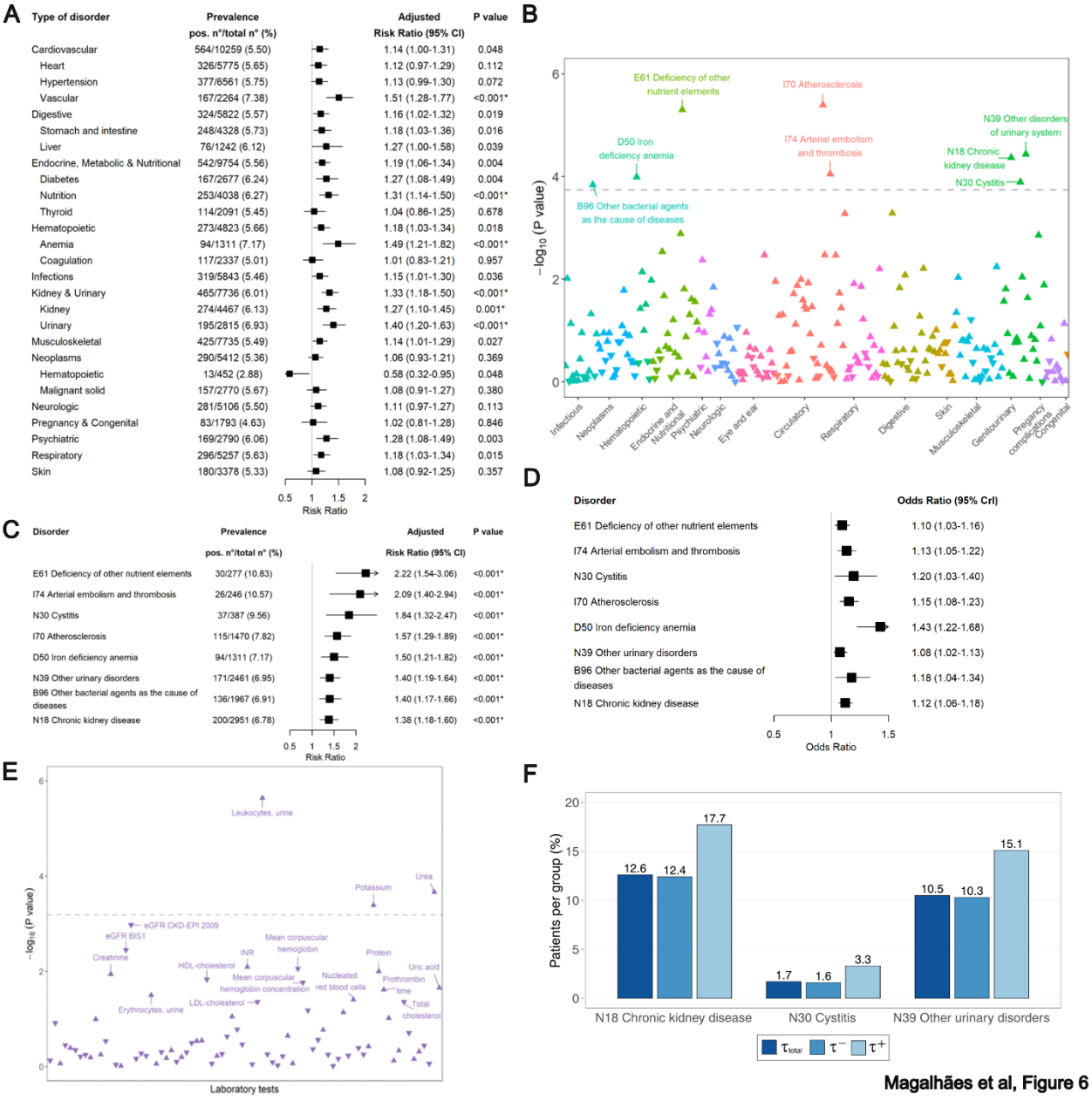

985 **Magalhães et al, Figure 6**

986 **Fig. 6. Association of MTBD-tau IgG autoantibodies and systemic disorders and clinical la-**
987 **boratory data. A.** Age- and sex-adjusted risk ratios ± 95% CI (bars) for $\alpha\tau^+$ autoantibodies
988 grouped 27 different main systemic clinical conditions. Asterisks: $P < 0.05$ after Bonferroni cor-
989 rection. **B.** $-\log_{10}$(P value) of the log-binomial regression for the presence of plasma MTBD-tau
990 IgG autoantibodies for 276 disorders according to ICD-10 codes and adjusted for age and sex.
991 Triangles pointing upwards and downwards: positive and coefficients, respectively; gray dashed
992 line: $P < 0.05$ after Bonferroni correction (here and henceforth). P values significant after Bonfer-

roni adjustment are labelled with the ICD codes. **C.** Same as (A), but according to individual disease entities from (B). **D**. Bayesian logistic regression adjusted for age and sex on ICD-10 codes significantly associated in B. and using -$\text{logit}_{10}(EC_{50})$ as continuous outcome (odds ratio ± 95% credible intervals). This analysis confirms the positive association of these ICD-10 codes with ατ reactivity (from B). **E.** -$\log_{10}$(P value) of the log-binomial regression for the presence of plasma MTBD-tau IgG autoantibodies and clinical laboratory parameters. P values significant after Bonferroni adjustment are labelled with the ICD codes. The gray dashed line indicates the significance level after Bonferroni correction (<0.05/106=0.00047). eGFR CKD-EPI 2009: estimated glomerular filtration rate using the Chronic Kidney Disease Epidemiology Collaboration 2009 equation; eGFR BIS1: estimated glomerular filtration rate using the older adults Berlin Initiative Study 1 equation. INR: international normalized ratio. LDL: low-density lipoprotein. HDL: high-density lipoprotein. **F.** Calculated prevalence of different ICD-10 codes in the total cohort (dark blue), $\alpha\tau^-$ (intermediate blue) and $\alpha\tau^+$ samples (light blue).